

Genome-wide variation study and inter-tissue communication analysis unveil regulatory mechanisms of egg-laying performance in chickens

Received: 10 December 2023

Accepted: 22 July 2024

Published online: 16 August 2024

 Check for updates

Dandan Wang ^{1,2}, Lizhi Tan ³, Yihao Zhi¹, Lina Bu³, Yangyang Wang¹, Zhang Wang ¹, Yulong Guo¹, Weihua Tian ¹, Chunlin Xu⁴, Donghua Li^{1,5}, Zhuanjian Li^{1,5}, Ruirui Jiang^{1,5}, Ruili Han^{1,5}, Guoxi Li^{1,5}, Yongqiang Wang², Dong Xia ⁶, Yadong Tian^{1,5}, Ian C. Dunn ⁷, Xiaoxiang Hu ³, Hong Li ^{1,5} ✉, Yiqiang Zhao ³ ✉, Xiangtao Kang ^{1,5} ✉ & Xiaojun Liu ^{1,5} ✉

Egg-laying performance is of great economic importance in poultry, but the underlying genetic mechanisms are still elusive. In this work, we conduct a multi-omics and multi-tissue integrative study in hens with distinct egg production, to detect the hub candidate genes and construct hub molecular networks contributing to egg-laying phenotypic differences. We identify three hub candidate genes as egg-laying facilitators: *TFPI2*, which promotes the GnRH secretion in hypothalamic neuron cells; *CAMK2D*, which promotes the FSH β and LH β secretion in pituitary cells; and *OSTN*, which promotes granulosa cell proliferation and the synthesis of sex steroid hormones. We reveal key endocrine factors involving egg production by inter-tissue crosstalk analysis, and demonstrate that both a hepatokine, APOA4, and an adipokine, ANGPTL2, could increase egg production by inter-tissue communication with hypothalamic-pituitary-ovarian axis. Together, These results reveal the molecular mechanisms of multi-tissue coordinative regulation of chicken egg-laying performance and provide key insights to avian reproductive regulation.

Egg production traits are economically most important in poultry industry. After a long-term breeding selection, the average annual egg numbers in the commercial layers have become significantly higher than that in the indigenous breed's¹. To understand the underlying genetic bases that control the egg-laying performance, many attempts have been made worldwide. A large number of genetic variants and more than 180 candidate genes have been discovered in different lines

and F2 resource populations based on quantitative trait loci mapping and genome-wide association study (GWAS)²⁻⁶, which were significantly associated with egg production traits such as age at first egg, egg number, laying rate and clutch size at the genomic level. However, the largest effect variation only accounted for 5.6% of the phenotypic variance of egg production traits⁷, and numerous other candidate genes and loci with small effects had yet to be mined.

¹College of Animal Science and Technology, Henan Agricultural University, Zhengzhou, China. ²College of Animal Science and Veterinary Medicine, Henan Institute of Science and Technology, Xinxiang, China. ³State Key Laboratory of Animal Biotech Breeding, College of Biological Sciences, China Agricultural University, Beijing, China. ⁴Henan Sangao Agriculture and Animal Husbandry Co, Ltd, Gushi, China. ⁵International Joint Research Laboratory for Poultry Breeding of Henan, Zhengzhou, China. ⁶Department of Pathobiology and Population Sciences, The Royal Veterinary College, London, UK. ⁷The Roslin Institute and Royal (Dick) School of Veterinary Studies, University of Edinburgh, Edinburgh, UK. ✉ e-mail: lihong19871202@163.com; yiqiangz@cau.edu.cn; xtkang2001@263.net; xjliu2008@hotmail.com

Meanwhile, selective sweep analyses among breeds with large phenotypic differences have been applied on exploration of the genomic regions and genes related to egg-laying performance^{18,9}. Comparative transcriptome analysis of tissues in hypothalamic-pituitary-ovarian (HPO) axis and different hierarchical follicles have identified a number of candidate genes and signaling pathways which potentially involved in reproductive development¹⁰, egg-laying difference¹¹, follicle selection, and reproductive hormone synthesis¹², providing potential bases for the regulatory mechanisms of egg-laying performance in chicken. However, only a few candidate genes known to be involved in reproductive regulation have been identified. Especially, some genetic causal genes have exhibited tissue bias¹³, which makes it difficult to identify the causal genes and molecular mechanisms that influence complex traits with just one of the above methods or single tissue¹³. The multi-tissue multi-omics systems biology approach could be more effectively at recognizing the causal genes affecting complex traits¹⁴, which provides a holistic understanding of the systemic complexity of organisms and deduces molecular interactions in the form of molecular networks from phenotypic related tissues¹⁴. This method has successfully facilitated the comprehensive analysis of human complex diseases and the detection of drug targets¹⁴.

In fact, egg production traits are the result of highly coordinated regulation of multiple tissues, which is not only directly controlled by HPO axis tissues, but also indirectly regulated by other peripheral tissues. Accumulated evidences have indicated that the liver and abdominal fat, as the vital tissues of energy storage and lipid dynamic changes, are closely related to the development and maturation of HPO axis and the deposition of vitelline materials, thus regulating egg-laying performance^{15,16}. It is noteworthy that the synergistic effects of multi-tissue on reproductive regulation are effectuated by inter-tissue signal communication¹⁷. Endocrine factors as a bridge between inter-tissue signal crosstalk have been investigated in many physiological aspects such as metabolism, immune system function and reproductive process^{18,19}. For instance, adiponectin (AdipoQ), an endocrine factor specifically secreted by mature adipocytes, could mediate hypothalamic gonadotropin-releasing hormone (GnRH) secretion and GnRH-induced pituitary luteinizing hormone (LH) release by targeting adiponectin receptors (AdipoR1 and AdipoR2) in the corresponding tissues²⁰. Therefore, systematic analysis of multi-tissue transcriptomes combined with other omics will be helpful to comprehensively analyze the molecular regulatory mechanisms of egg production in poultry.

In this work, we first conduct multi-method GWAS and selective sweep analysis based on multi-breed genome resequencing to identify genetic signals and candidate genes involving egg production traits. Subsequently, we perform multi-tissue comparative transcriptome analyses of hypothalamus, pituitary, ovary, liver, and abdominal fat between high- and low-yield chickens. The laying-related hub candidate genes (HCGs) are systematically excavated by integrative analysis of the above genomic and transcriptome studies. We then employ the Quantitative Endocrine Network Interaction Estimation (QENIE) strategy to identify laying-related key endocrine factors. Furthermore, we construct the molecular regulatory networks of HCGs within multiple tissues, verify their function in primary cells of tissues in HPO axis, and explore the inter-tissue communication mechanism of key endocrine factors regulating egg production via the tissue-specific over-expression in vivo. Our findings provide a synergistic and interacting molecular network and regulatory mechanism of egg-laying performance in chickens, and will broaden the perspective of exploring genetic bases of other complex traits.

Results

Potential genetic variants and gene sets involving egg production

We resequenced 900 individuals of Gushi chicken with large phenotypic variations in egg production (the coefficient of variance from

11.17% to 75.05% across different traits) to trace the genetic signals association with egg production traits, including egg number (EN) at different laying periods (EN21-25w, EN26-30w, EN31-35w, EN36-43w, EN31-43w and ENT), average clutch size (ACS) at different laying periods (ACS21-25w, ACS26-30w, ACS31-35w, ACS36-43w, ACS31-43w and ACST) and maximum clutch size (MCS) (Supplementary Table 1). After quality control and filtration, a total of 13,467,604 autosomal SNPs from 888 individuals were obtained. The SNP-based heritability was estimated ranging from 0.05 to 0.42 over the thirteen egg production traits (Supplementary Data 1). A strong genetic positive correlation was observed among egg number and clutch size, and the genetic correlation coefficients range from 0.56 to 1.00 (Supplementary Data 1).

Further, we combined the univariate SNP-based GWAS, the univariate haplotype-based GWAS (hap-based GWAS), and the multivariate canonical correlation analysis (CCA)-based GWAS to uncover the potential small-effect and pleiotropic variants and gene sets related to egg production traits in Gushi chicken. Multiple signaling regions located on autosomes were identified, some of which were co-located by multiple egg production traits or by multiple GWAS methods (Fig. 1, Supplementary Figs. 1, 2). For instance, a 580 kb region located on GGA3 (108.04–108.62 Mb) was identified by SNP-based GWAS (EN21-25w, EN36-43w, and ENT), which contained two genes *TFAP2B* and *TFAP2D* (Supplementary Fig. 3a). A 40 kb region located on GGA24 (4.19–4.23 Mb) was identified across SNP-based GWAS (EN31-43w, ACS31-43w and ACST), haplotype-based GWAS (EN31-43w, ENT, ACS31-43w, ACST, and MCS), and CCA-based GWAS (CS), which contained four genes *THY1*, *USP2*, *MFRP* and *CIQTNF5* (Supplementary Fig. 3b). Of the six genes, *TFAP2D* and *THY1* were previously identified as the candidate genes related to 500-day egg number in a native chicken⁴, and related to 196–227-day egg number in meat-type chicken⁶, respectively.

Overall, the SNP-based GWAS approach revealed the potential 72 large-effect ($P < 1.01E-06$) and 4981 small-effect SNPs ($1.01E-06 < P < 1.00E-04$) (Supplementary Data 2), and the haplotype-based GWAS approach revealed the potential 251 large-effect and 8007 small-effect haplotypes on egg production traits (Supplementary Data 3). The total effects of the potential 5053 SNPs and 8258 haplotypes could explain 37.41–64.46% and 35.99–63.50% of phenotypic variances of different egg production traits, respectively (Supplementary Table 2). The CCA-based GWAS approach identified the potential 176 large-effect and 3530 small-effect SNPs for EN, clutch size (CS) or all EN and CS (all-EN-CS) (Supplementary Data 4). Focusing on the upstream and downstream 50 kb genomic regions of all these potential SNPs and haplotypes, we annotated 4668 (SNP-GWASGs), 6683 (hap-GWASGs), and 4071 (CCA-GWASGs) genes within these genomic intervals in SNP-based GWAS, haplotype-based GWAS and CCA-based GWAS, respectively (Supplementary Data 5). Of these genes, 105 overlapped with the previously reported 213 candidate genes (213 RCGs from 2011 to 2023) that were significantly associated with EN, laying rate (LR), age at first egg (AFE), number of clutches (numC) and longest clutch (LC)²⁻⁷ (Supplementary Data 6, Supplementary Fig. 4). Some overlapped candidate genes such as follicle-stimulating hormone receptor (*FSHR*), growth differentiation factor 9 (*GDF9*), estrogen receptor 1 (*ESR1*), estrogen receptor 2 (*ESR2*), matrix metalloproteinase 13 (*MMP13*), luteinizing hormone/choriogonadotropin receptor (*LHCGR*), prolactin-releasing hormone receptor (*PRLHR*) and neurexin 1 (*NRXN1*), which have been reported to function in regulating chicken reproduction².

Selective regions and genes related to layer breed formation

Modern chicken breeds are primarily domesticated from the red jungle fowl⁹. There was a long process of early domestication and later phenotypic-oriented breeding of varieties or lines, which resulted in a rapid increase in the egg production, from 5-9 eggs per year in red jungle fowl to over 300 eggs per year in modern

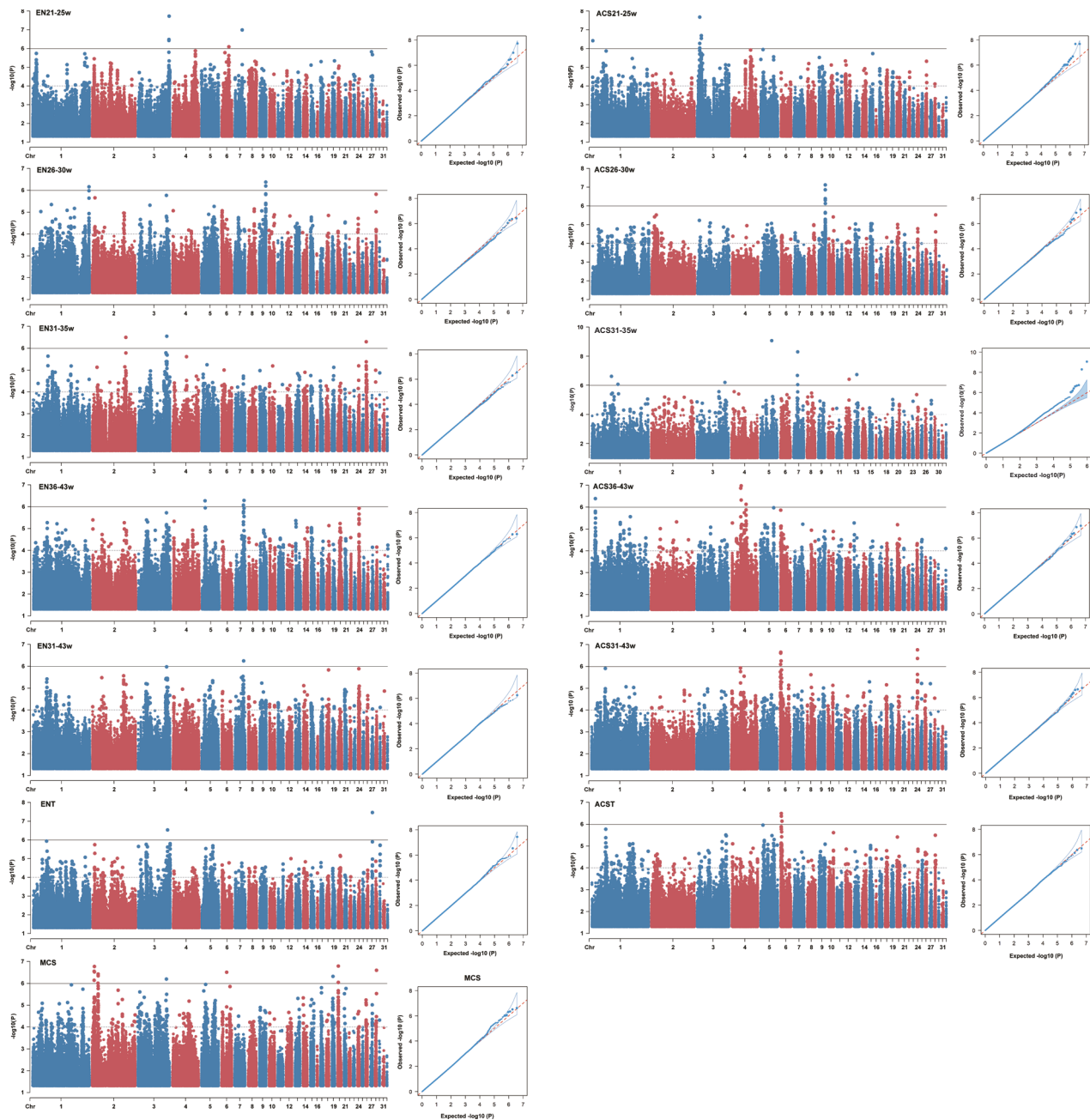


Fig. 1 | Manhattan and quantile-quantile (Q-Q) plots of SNP-based whole-genome association signals for egg production traits in Gushi chicken. Association testing was performed using linear mixed model. Association testing was performed using linear mixed model. The significance was corrected by a relaxed correction for multiple comparisons and was self-defined as the large effect significance threshold ($P = 1/(\text{SNP numbers})$; $-\log_{10}(P) = 6$; the horizontal solid line) or small effect significance threshold ($-\log_{10}(P) = 4$; the horizontal dashed line).

$N = 888$ individuals. EN21-25w, EN26-30w, EN31-35w, EN36-43w, EN31-43w represent egg number at 21–25 weeks of age, 26–30 weeks of age, 31–35 weeks of age, 36–43 weeks of age, 31–43 weeks of age, respectively. ENT represents total egg number. MCS represents maximum clutch size. ACS21-25w, ACS26-30w, ACS31-35w, ACS36-43w, and ACS31-43w represent average clutch size in each of five stages consistent with the statistical stage division of egg number. ACST represents total average clutch size.

commercial layers¹. To detect genes that were subject to genetic selection during domestication or breeding associated with egg-laying phenotype, 20 wild ancestors^{1,21}, 50 native birds²² and 20 layers¹ (Supplementary Data 7) were collected for comparative genomic analysis. A total of 14.65 Gb high-quality clean reads was generated with an average sequencing depth of 13.82 \times coverage per individual (Supplementary Data 7). After filtration, a final set of 16.95 million SNPs (Supplementary Data 8) was obtained. A comprehensive analysis of genetic relationships among these breeds was conducted. As expected, phylogenetic analysis and principal component analysis

(PCA) divided wild ancestors, native chickens, and commercial layers into separate clusters (Fig. 2a, b). The commercial layer breeds had a sizeable genetic difference with native chicken breeds or wild ancestors. Additionally, two layer breeds were also separated, possibly due to the considerable differences in other physiological characteristics, such as body weight (White Leghorn hen weigh around 1.8 kg, while Rhode Island Red hen weigh around 2.9 kg), the different geographical locations and various artificial selection intensities⁹ (Supplementary Fig. 5). LD decay analysis proved a stronger selection pressure on layer breed chickens (Fig. 2c).

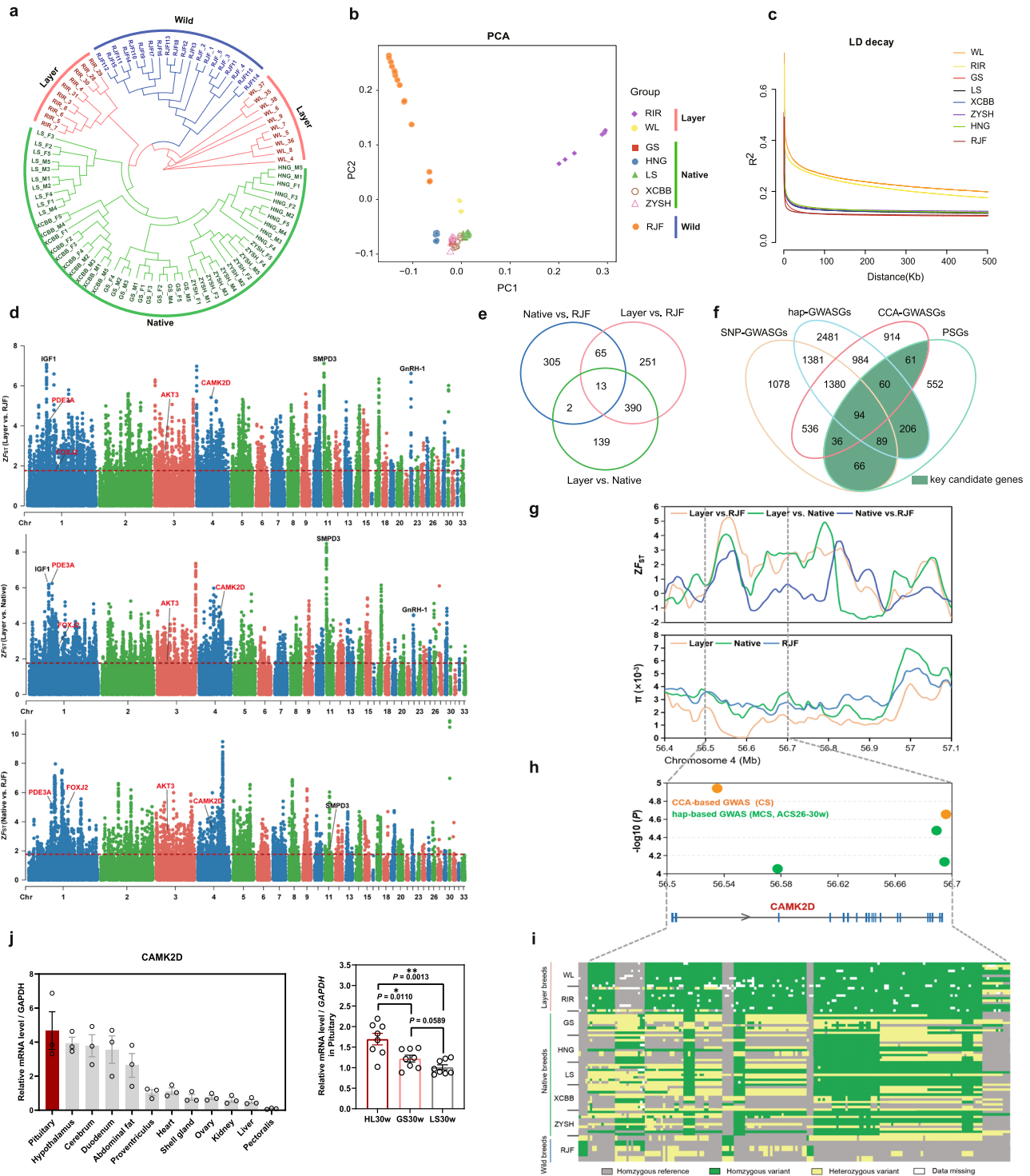


Fig. 2 | Comparative genomic analysis revealed selective regions and genes related to layer breed formation. **a** Phylogenetic tree analysis of different breeds. **b** Principal component analysis of different breeds. **c** Linkage disequilibrium decay analysis of different breeds. **d** Selective signals of layer vs. RJF, layer vs. native and native vs. RJF based on $Z_{F_{ST}}$ analysis. The horizontal red dashed lines correspond to the top 5% threshold. **e** Venn diagram of potential selected genes (PSGs) in three comparison groups. **f** Venn diagram of the intersection of GWASGs and PSGs. **g** Selective signals of *CAMK2D* in the three comparison groups. **h** SNPs and haplotypes in *CAMK2D* significantly associated with egg production traits in Gushi chicken. Chi-square test and F-test were performed to assess the association significance in CCA-based GWAS and haplotype-based GWAS, respectively. CS represents clutch size, MCS represents maximum clutch size, and ACS26-30w represents average clutch size from 31 to 43 weeks of age. **i** The genotype pattern of SNPs located in the promoter and intron regions of *CAMK2D*. **j** Tissue expression pattern of *CAMK2D* in 30-week-old Hy-line layers and native chickens ($n = 3$ for the expression in different tissues; $n = 8$ for the expression in different breeds). Layer: WL (White Leghorn) and RIR (Rhode Island Red). Native chicken breeds: Gushi (GS), Lushi (LS), Xichuan Black Bone (XCBB), Zhengyang San Huang (ZYSH) and Henan Gamecock (HNG) chickens. Wild breed: RJF (Red Jungle Fowl). The data for (j) are presented as the mean \pm SEM, and the indicated P values ($*P < 0.05$, $**P < 0.01$) are based on two-tailed unpaired t-test. Source data are provided as a Source Data file.

represents clutch size, MCS represents maximum clutch size, and ACS26-30w represents average clutch size from 31 to 43 weeks of age. **i** The genotype pattern of SNPs located in the promoter and intron regions of *CAMK2D*. **j** Tissue expression pattern of *CAMK2D* in 30-week-old Hy-line layers and native chickens ($n = 3$ for the expression in different tissues; $n = 8$ for the expression in different breeds). Layer: WL (White Leghorn) and RIR (Rhode Island Red). Native chicken breeds: Gushi (GS), Lushi (LS), Xichuan Black Bone (XCBB), Zhengyang San Huang (ZYSH) and Henan Gamecock (HNG) chickens. Wild breed: RJF (Red Jungle Fowl). The data for (j) are presented as the mean \pm SEM, and the indicated P values ($*P < 0.05$, $**P < 0.01$) are based on two-tailed unpaired t-test. Source data are provided as a Source Data file.

To detect the potential genomic selective regions (PGSRs) on autosomes in the formation of layer breeds, we scanned the genome for regions with the high population genetic differentiation (F_{ST}) and the high differences in genetic diversity (π -ratio) in 40-kb sliding windows in native vs. RJF, layer vs. native, and layer vs. RJF comparison groups. In total, we identified 821 PGSRs (top 5% signals, with Z-transformed F_{ST} (ZF_{ST}) > 1.77 and $\log_2(\pi\text{-ratio}) < -0.17$) covering or being near to 385 potential selective genes (PSGs) in native vs. RJF group, 974 PGSRs (ZF_{ST} > 1.84 and $\log_2(\pi\text{-ratio}) < -0.86$) carrying 544 PSGs in layer vs. native group, and 1390 PGSRs (ZF_{ST} > 1.82 and $\log_2(\pi\text{-ratio}) < -0.73$) carrying 719 PSGs in layer vs. RJF group, respectively (Fig. 2d, Supplementary Fig. 6, Supplementary Data 9–11). In these selection analyses, several PSGs associated with body size²³ (insulin-like growth factor 1, *IGF1*, ZF_{ST} = 6.05), muscle development²⁴ (sphingomyelin phosphodiesterase 3, *SMPD3*, ZF_{ST} = 8.48) and reproductive processes¹⁹ (gonadotropin-releasing hormone 1, *GnRH-1*, ZF_{ST} = 6.61) were strongly selected in layers and overlapped with previously detected genomic sweep regions (Fig. 2d). Combined with all selection analyses of three comparison groups, a total of 1165 PSGs were detected as potential regulators of phenotypic traits in the formation of layer breed (Fig. 2e, Supplementary Data 12).

Key candidate genes affecting egg production

By comparing the gene lists between GWASs and PSGs, 612 overlapping genes that were strongly selected and significantly associated with egg production traits were screened as key candidate genes (KCGs) affecting chicken egg production at different stages (Fig. 2f, Supplementary Data 13). These KCGs mainly involved in regulation of system process ($-\log_{10}(Q) = 1.67$), transport of small molecules ($-\log_{10}(Q) = 1.67$), regulation of cellular response to stress ($-\log_{10}(Q) = 1.67$), intermembrane lipid transfer ($-\log_{10}(Q) = 1.67$) and regulation of protein-containing complex disassembly ($-\log_{10}(Q) = 1.67$) (Supplementary Fig. 7).

Of the 612 KCGs, 12 genes were subjected to the consistent selection in domestication and improvement stages, among which four genes, including calcium/calmodulin dependent protein kinase II delta (*CAMK2D*)²⁵, phosphodiesterase 3A (*PDE3A*)²⁶, AKT serine/threonine kinase 3 (*AKT3*)²⁷, and forkhead box J3 (*FOXJ2*)²⁸ were reported to be associated with reproductive regulation (Fig. 2d, Supplementary Data 14). The *CAMK2D* were involved in calcium signaling pathway that mobilized Ca^{2+} stores and GnRH signaling pathway that facilitated the expression and secretion of LH and FSH in mouse²⁵, but its function in poultry was unclear. Additionally, SNPs genotypes of *CAMK2D* were nearly fixed in layer breeds ($\pi_{layer} = 3.87E-05$) (Fig. 2g), and the SNPs and haplotypes in *CAMK2D* was mainly associated with clutch size including CS, ACS26-30w and MCS in Gushi chickens ($4 < -\log_{10}(P) \leq 4.88$) (Fig. 2h). The genotype pattern of variants located in the promoter and intron regions of *CAMK2D* gene were different among RJF, native breeds, and layer breeds (Fig. 2i). Real-time quantitative PCR (qRT-PCR) analysis showed that *CAMK2D* was highly expressed in the pituitary of 30-week-old hens, and a highest expression level in the pituitary of high-yield Hy-Line layers, followed by the low-yield native chicken breeds (GS and LS chicken) (Fig. 2j). Furthermore, GnRH induced the up-regulation of *CAMK2D* expression in chicken pituitary cells, thus promoting the synthesis and secretion of FSH β and LH β in pituitary to positively regulate egg production in chicken (Supplementary Fig. 8).

Molecular networks driving the differences in egg production

Egg production trait is a typical complex trait involving multiple tissues regulation, including HPO axis, liver, and abdominal fat^{15,16}. Here, we tracked the egg-laying phenotypes of Gushi hens in the 14th generation at 20, 28, 36, and 43 weeks of age, including EN, reproductive hormone levels, liver index (LI), abdominal fat percentage (AFP), ovarian weight (OW) and ovarian follicle numbers (Supplementary Fig. 9, 10,

Supplementary Data 15, 16), and found that the decrease of EN in decline laying stage (GS36w and GS43w) was significantly correlated with the increase of LI and AFP ($P < 0.05$), whereas OW only affected early egg production (GS20w) ($P < 0.05$) (Supplementary Data 16).

To construct and excavate the hub molecular networks that regulate egg production via synergistic interaction of multi-tissues, we then collected five tissues including hypothalamus, pituitary, ovary, liver and abdominal fat of high- and low-yield hens at 43 weeks of age, respectively, for transcriptome analyses. We constructed 78 mRNA libraries, and generated a total of 561.91 Gb high-quality RNA-seq data (~7.20 Gb sequences per sample) (Supplementary Data 17). A total of 17,063 genes including 14,487 annotated genes and 2576 unannotated genes were expressed in the five tissues. The PCA clearly distinguished the five tissues, but did not completely separate the high- and low-yield group (Fig. 3a).

Using weighted gene co-expression network analysis (WGCNA), we detected hub genes that were significantly associated with egg-laying related phenotypes (Fig. 3b). The EN39-43w and ENT, as well as the serum concentrations of FSH, LH, PROG, and E2 were used for WGCNA (Fig. 3c, Supplementary Fig. 11). A total of 13 significant modules ($P < 0.05$) including 2425 module hub genes (MHGs) were positively correlated with egg production (designated as pMHGs), including 472 in the hypothalamus, 174 in the pituitary, 831 in the ovary, 870 in the liver and 303 in the abdominal fat (Fig. 3c, Supplementary Data 18). Meanwhile, a total of 25 significant modules ($P < 0.05$) including 7088 MHGs were negatively correlated with egg production (designated as nMHGs), including 919 in the hypothalamus, 2372 in the pituitary, 3277 in the ovary, 1385 in the liver and 1011 in the abdominal fat (Supplementary Data 19). Furthermore, a total of 106, 225, 1191, 1030, and 886 differentially expressed genes (DEGs) were detected in the hypothalamus, pituitary, ovary, liver, and abdominal fat between high- and low-yield hens (Fig. 3d, Supplementary Fig. 12, Supplementary Data 20). By integrating the DEGs with 2425 pMHGs and 7088 nMHGs (Fig. 3e), a total of 628 differential pMHGs (DpMHGs) (Supplementary Data 21) and 1075 differential nMHGs (DnMHGs) (Supplementary Data 22) were obtained, which contained 24 positive and 30 negative KCGs, defined as HCGs, driving the egg-laying phenotypic differences, respectively (Fig. 3f, Supplementary Tables 3, 4). The significant differences in the expression of 3 HCGs (*TFPI2*, *TPPA*, and *ADGRG2*) in hypothalamus and 6 HCGs (*OSTN*, *ANK2*, *ILIRL1*, *ANOS*, *ADGRF5*, and *PLXDC2*) in ovary of high- and low-yield hens were verified by qRT-PCR (Supplementary Fig. 13).

Based on the co-expression relationships of DpMHGs and DnMHGs in the WGCNA modules, we constructed HCGs co-expression regulatory networks in each of the five tissues (Fig. 4a, Supplementary Figs. 14, 15). Based on GO annotation, the functional enrichments of HCGs and its linked co-expression DpMHGs or DnMHGs were tissue-specific. For example, the different positive HCGs co-expression networks were mainly involved in regulating carboxylic acid biosynthetic process and amyloid-beta clearance in hypothalamus (gray modules), luteinizing hormone secretion, intracellular transport and JAK-STAT cascade in pituitary (white modules), as well as extracellular matrix organization and transmembrane receptor protein serine/threonine kinase signaling pathway in ovary (lightpink4 modules) (Fig. 4a). Additionally, we observed that the gene connectivity of most HCGs was not as high as that of other DpMHGs or DnMHGs, that is, most of HCGs was not at the core of the regulatory networks. This echoed the hypothesis of “omnigenic” model that for any given complex phenotype, most genes with genetic effects are distributed in the periphery of core genes and collectively drive phenotypic changes through sufficiently interconnected gene regulatory networks²⁹.

Functional validation of HCGs in the HPO axis in vitro

We investigated the function of HCGs in primary cells from the positive regulatory network of the HPO axis, which drove female follicular

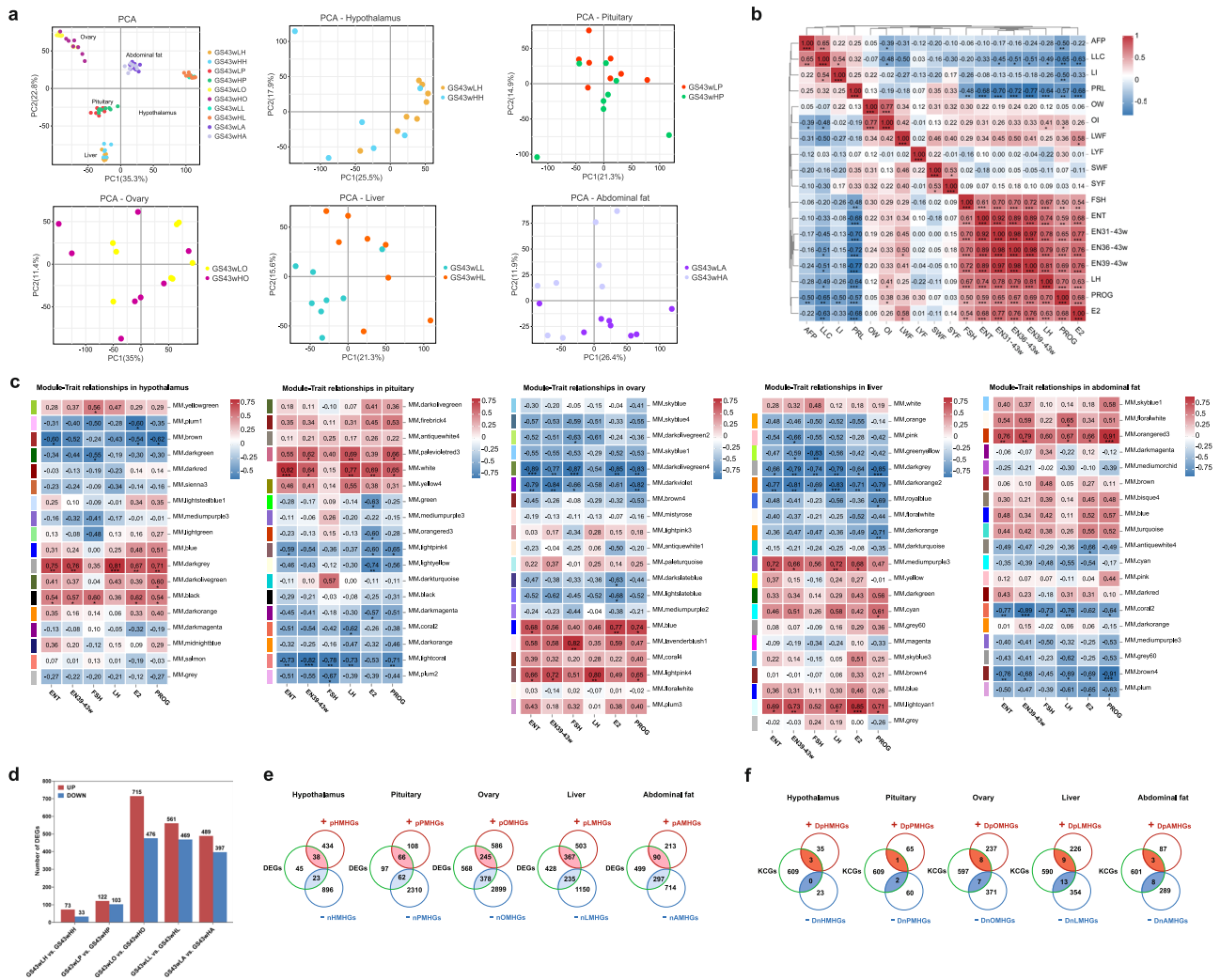


Fig. 3 | Multi-tissue transcriptome analysis excavated hub candidate genes regulating egg production. **a** Principal component analysis of sequencing samples from 5 tissues. GS43wLH and GS43wHH represent the low- and high-yield groups of 43-week-old Gushi chickens in hypothalamus, respectively. The classification of other tissues are similar to the hypothalamus. **b** Pearson correlation analysis of all phenotypes in 43-week-old Gushi chickens. AFP, LLC, LI, OW, and OI represent abdominal fat percentage, liver lipid content, liver index, ovarian weight and ovarian index, respectively. **c** Module-egg production traits relationships in five tissues. **d** Differentially expressed genes (DEGs) obtained by comparing high-

and low-yield groups of different tissues. **e** The intersection of DEGs and module hub genes (MHGs). pMHGs represent the MHGs positively correlated with egg production in hypothalamus. nMHGs represent the MHGs negatively correlated with egg production in hypothalamus. The representation of MHGs in other tissues is similar to that in hypothalamus. **f** The intersection of key candidate genes (KCGs) and differential MHGs. The data in (**b**, **c**) are presented as the correlation coefficient ($*P < 0.05$; $**P < 0.01$ and $***P < 0.001$) were performed by two-tailed unpaired *t*-test.

development, egg maturation, and ovulation³⁰. In hypothalamus, we performed functional validation for the tissue factor pathway inhibitor 2 gene (*TFPI2*) (Fig. 4a), which was located on the selective region of GGA2 (23.3–23.4 Mb) (ZF_{ST} (Max) = 2.35 in native vs. RJF, ZF_{ST} (Max) = 1.81 in layer vs. RJF), and was significantly associated with ACS31-35w, ACS31-43w and ACST in hap-based GWAS method and CS in CCA-based GWAS in Gushi chickens ($4 < -\log_{10}(P) \leq 5.05$) (Supplementary Fig. 16). We first confirmed that the mRNA level of *TFPI2* were significantly higher in hypothalamus of high-yield group compared with that of low-yield group in Gushi chickens at 28, 36, and 43 weeks of age ($P \leq 0.05$, Fig. 4b). Functional gain and loss assays of *TFPI2* in chicken primary hypothalamic neuron cells indicated that *TFPI2* could reduce the expression level of neuropeptide VF precursor (*NPVF*, also named GnIH, a gonadotropin-inhibiting hormone) and promote the secretion of GnRH, but had no effect on *GnRH* expression (Supplementary Fig. 17, Fig. 4c), which confirmed the regulatory function of *TFPI2* on the secretion of the hypothalamic reproductive hormone GnRH. We also observed the response patterns of *TFPI2*-adjacent genes such as

FK506 binding protein 5 (*FKBP5*), asparaginase (*ASPG*), and solute carrier family 38 member 4 (*SLC38A4*) in the regulatory network. The result showed that all of these genes exhibited up-regulated expression upon *TFPI2* overexpression and knockdown (Supplementary Fig. 18).

In ovary, we also performed functional validation for osteocrin gene (*OSTN*) (Fig. 4a), which was located on the selective region of GGA9 (13.7–14.0 Mb) (ZF_{ST} (Max) = 4.55 in layer vs. RJF, ZF_{ST} (Max) = 3.97 in layer vs. native), and was significantly associated with multiple egg production traits including EN26-30w, EN31-35w, EN36-43w, EN31-43w, ACS21-25w, ACS26-30w, ACST, MCS, CS and all-EN-CS across multiple GWAS methods in Gushi chickens ($4 < -\log_{10}(P) \leq 6.87$) (Supplementary Fig. 19). *OSTN* expression was significantly higher in ovary tissue of high-yield group than low-yield group at 20, 36, and 43 weeks of age (Fig. 4d). Functional gain and loss assays of *OSTN* gene in chicken ovarian granulosa cells (GCs) showed that *OSTN* could promote the expression of mRNA and protein levels of steroid hormone synthesis pathway genes (steroidogenic acute regulatory

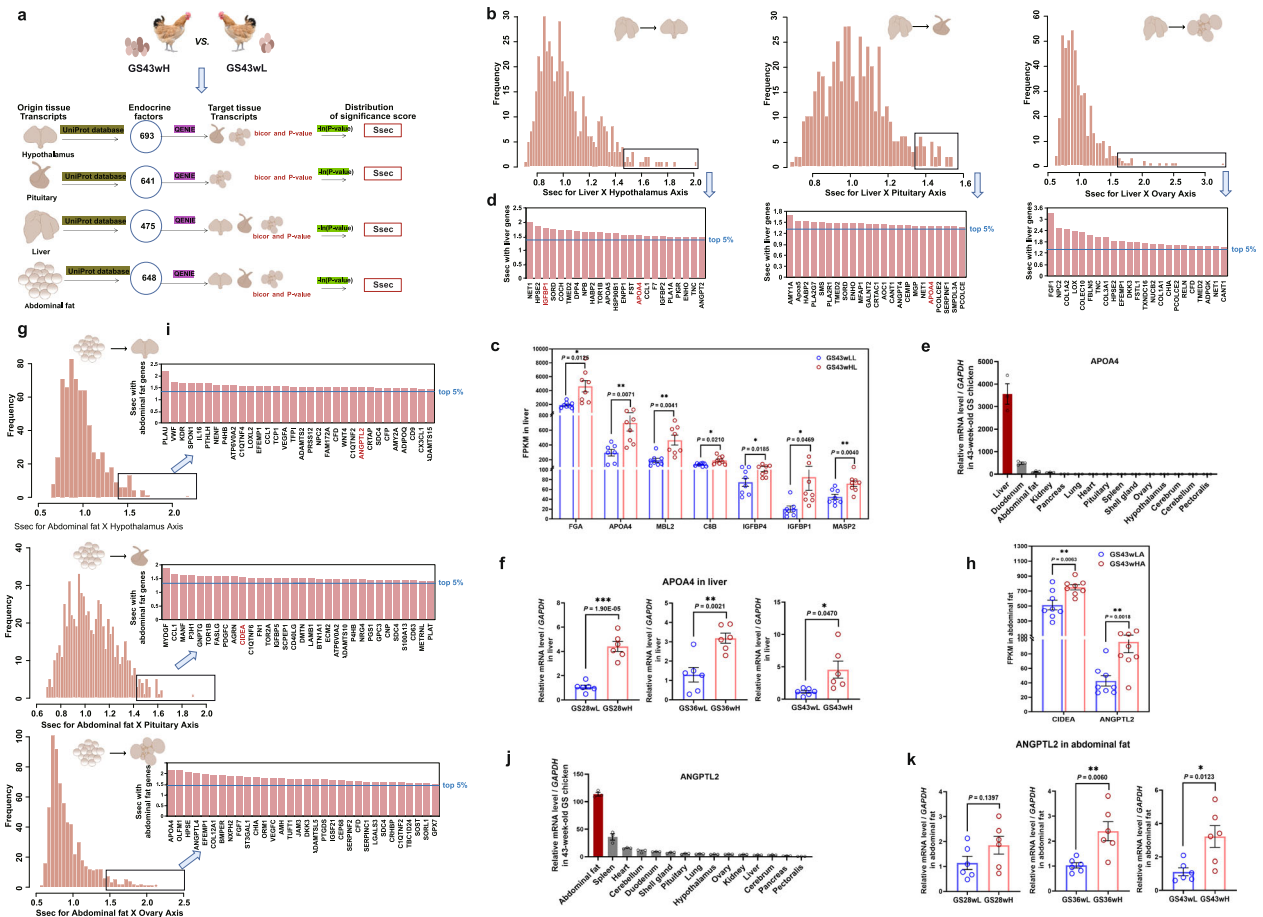


Fig. 5 | Multi-tissue systematic screening for key endocrine factors of inter-tissue crosstalk regulating egg production in chicken. **a** Flow chart of inter-tissue crosstalk analysis. **b** Rank of all liver endocrine factors based on Ssec of liver-HPO axis crosstalk. **c** FPKM of liver-specific endocrine factors in the liver of 43-week-old Gushi chickens in high- (GS43wHL) and low-yield groups (GS43wLL) ($n = 7-8$ for each group). **d** Liver endocrine factors of top 5% Ssec. **e** Expression of *APOA4* in different tissues of 43-week-old Gushi chickens ($n = 3$). **f** Expression difference of *APOA4* in high- and low-yield groups at different laying stages ($n = 6$ for each group). **g** Rank of all abdominal fat endocrine factors based on Ssec of abdominal fat-HPO axis crosstalk. **h** FPKM of abdominal fat-specific endocrine factors in the abdominal fat of 43-week-old Gushi chickens in high- (GS43wHA) and

low-yield groups (GS43wLA) ($n = 8$ for each group). **i** Abdominal fat endocrine factors of top 5% Ssec. **j** Expression of *ANGPTL2* in different tissues of 43-week-old Gushi chickens ($n = 3$). **k** Expression difference of *ANGPTL2* in high- and low-yield groups at different laying stages ($n = 6$ for each group). Ssec indicates the strength of cross-tissue predictions for endocrine circuits. GS28wL and GS28wH, GS36wL and GS36wH, GS43wL and GS43wH, represent the high- and low-yield groups of Gushi chickens at 28, 36, and 43 weeks of age, respectively. The data in (c, e, f, h, j, k) are presented as the mean \pm SEM; groups with significant differences ($*P < 0.05$, $**P < 0.01$, and $***P < 0.001$) were performed by two-tailed unpaired t-test. Source data for are provided as a Source Data file.

coincided with those of *OSTN* in the GCs (Supplementary Fig. 22). These results suggested that *OSTN* gene perhaps positively affect egg production by interconnecting with other genes to promote the synthesis and secretion of PROG and E2 hormones in granulosa cells and the follicle growth.

Key endocrine factors regulating egg production via inter-tissue crosstalk

As organism is a whole coordinately regulated by multiple tissue systems, in addition to intra-tissue signaling, the inter-tissue crosstalk also plays an indispensable role in reproduction regulation. We systematically screened the key endocrine factors of inter-tissue crosstalk regulating egg production in chickens using a QENIE approach. All transcriptome data from the above five tissues of high- and low-yield Gushi chickens were used to detect the correlations between endocrine factors secreted from hypothalamus, pituitary, liver, and abdominal fat, and their response genes in HPO axis tissues (Fig. 5a). A total of 693, 641, 475, and 648 endocrine factors were identified in the hypothalamus, pituitary, liver, and abdominal fat based on the Universal Protein Resource (UniProt) database, respectively

(Supplementary Data 23). We constructed endocrine circuits of tissue pairs and assessed strength of cross-tissue predictions for endocrine circuits, termed Ssec. We generated the Ssec lists of potential mediators of origin-target tissue pair (top 100) (Supplementary Data 24–26). A total of 35 hypothalamus-specific and 7 pituitary-specific endocrine factors were identified (Supplementary Fig. 23). However, only 27 out of 35 showed differential expression in the hypothalamus between high- and low-yield groups (Supplementary Fig. 24), and were considered as key hypothalamic endocrine factors. Among the 27 hypothalamus-specific endocrine factors, some were well documented about their reproductive regulatory functions, such as vasoactive intestinal polypeptide (*VIP*)³³, proenkephalin (*PENK*)³⁴, and gremlin 2 (*GREM2*)³⁵. Some were involved in food intake and energy metabolism, such as neuropeptide Y (*NPY*)³⁶, pancreatic polypeptide (*PPY*)³⁷, orphenkephalin precursor (*PNOC*)³⁸, galanin and GMAP prepeptide (*GAL*)³⁹, and neuroregulatory peptide receptor (*NMU*)⁴⁰. This suggested that endocrine factors coordinated the dynamics of energy metabolism and reproduction in the hypothalamus. Interestingly, some secreted proteins such as growth and differentiation factor 10 (*GDF10*)⁴¹ and Wnt inhibitory factor 1 (*WIF1*)⁴² were also identified,

which suggesting their potential role in regulating egg production through different pathways.

For the liver-HPO axis tissue pairs, 38 liver-specific endocrine factors were identified (Fig. 5b, Supplementary Fig. 25). Fifteen of the 38 liver-endocrine factors were significantly differentially expressed in the liver between high- and low-yield groups, including 7 positively and 8 negatively correlated with egg-laying phenotypes (Fig. 5c, Supplementary Fig. 26), thus were selected as the key endocrine factors of liver-HPO axis communication. Among the 7 key endocrine factors positively correlated with egg-laying phenotypes (Fig. 5c), apolipoprotein A4 (*APOA4*) ranked top among the three tissue pairs corresponding to liver (top 5% Ssec in liver-hypothalamus, top 5% Ssec in liver-pituitary, and top 15% Ssec in liver-ovary) (Fig. 5d, Supplementary Data 25), and was significantly associated with egg production at multiple laying stages (Fig. 5e, f), so was used for subsequent functional validation.

For the abdominal fat-HPO axis tissue pairs, we identified a total of 35 abdominal fat-specific endocrine factors (Fig. 5g, Supplementary Fig. 27), among which, 19 were differentially expressed in abdominal fat between high- and low-yield groups (Fig. 5h, Supplementary Fig. 28), thus was selected as the key endocrine factors of abdominal fat-HPO axis communication. Among the 19 abdominal fat-specific endocrine factors, only angiopoietin-like 2 gene (*ANGPTL2*) from abdominal fat-hypothalamus pair and cell death-inducing DFFA-like effector a gene (*CIDEA*) from abdominal fat-pituitary pair were positively related to egg production (Fig. 5h) and ranked top 5% Ssec (Fig. 5i), suggesting that most of abdominal fat-specific endocrine factors in late laying period were not conducive to egg production. The *ANGPTL2* was significantly highly expressed in the abdominal fat and associated with egg production at multiple laying stages (Fig. 5j, k), thus was a candidate used for function test in abdominal fat-hypothalamus communication.

Peripheral tissue-HPO axis crosstalk improves egg production

To further verify the regulatory effects of liver-specific and abdominal fat-specific endocrine factors on egg production, we constructed liver-specific *APOA4* overexpressed adeno-associated virus (AAV9-*APOA4*) and abdominal fat-specific *ANGPTL2* overexpressed adeno-associated virus (AAV9-*ANGPTL2*) and injected them into 12-week-old Gushi pullets, respectively. We tracked the expressions of liver-specific *APOA4* and abdominal fat-specific *ANGPTL2* in each group and determined the changes in the egg-laying related phenotypes after 10 weeks.

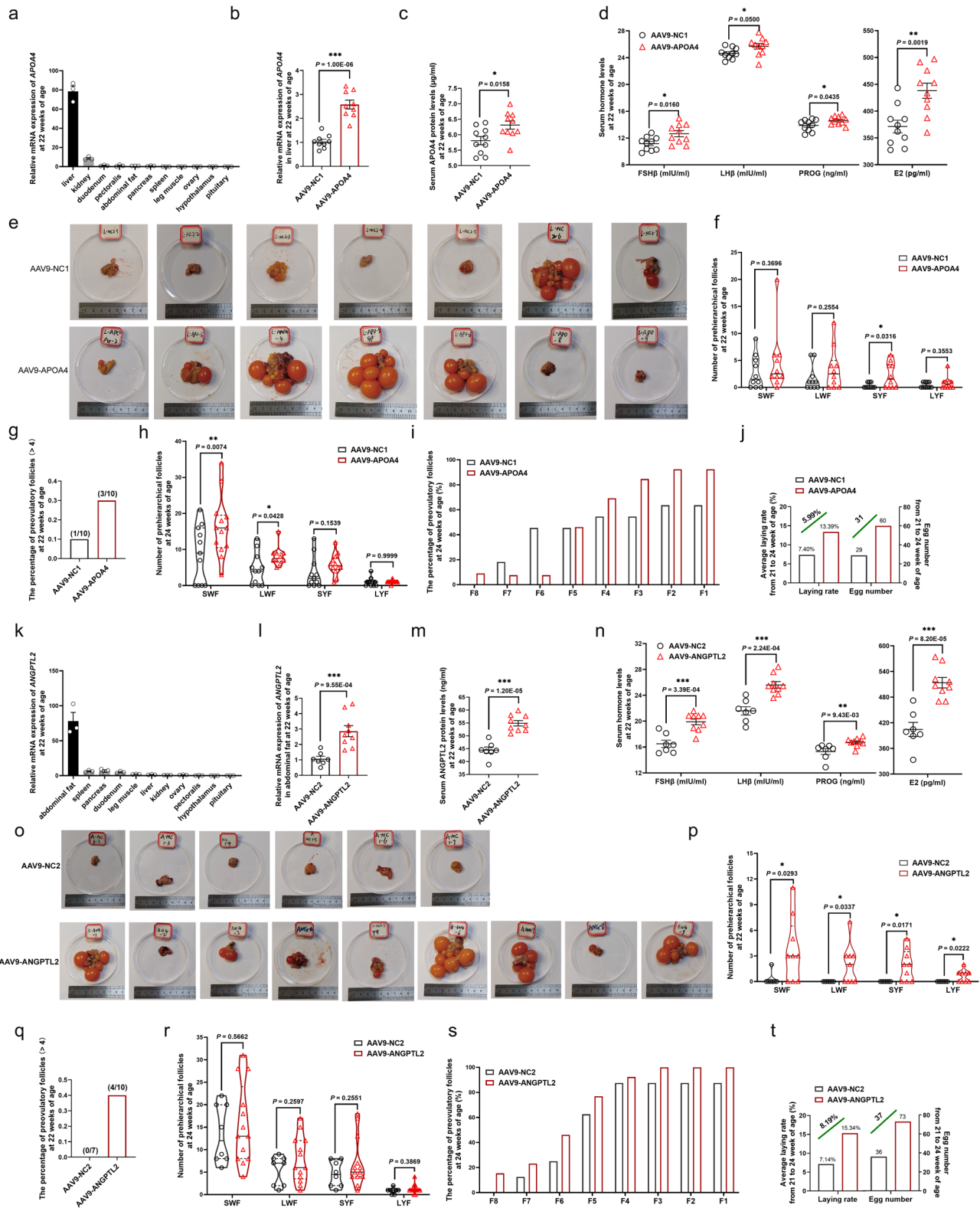
The liver-specific expression of *APOA4* was reconfirmed in AAV9-*APOA4* group of 22-week-old Gushi hens (Fig. 6a). Both hepatic *APOA4* mRNA level and serum *APOA4* protein level in AAV9-*APOA4* group at 22 weeks of age were obviously elevated compared with AAV9-NC1 group (Fig. 6b and c), indicating that *APOA4* was successfully liver-specific overexpressed in vivo. Hens receiving AAV9-*APOA4* virus had higher serum reproductive hormone levels (FSH β , LH β , E2, and PROG) than those receiving AAV9-NC1 virus at 22 weeks of age (Fig. 6d). Interestingly, *APOA4* overexpression did not affect body weight and liver index (LI) but decreased abdominal fat percentage (AFP) of hens ($P = 0.0037$ in 22 weeks, $P = 0.1416$ in 24 weeks) at 22 and 24 weeks of age (Supplementary Fig. 29). In addition, *APOA4* overexpression increased ovary index (OI) ($P = 0.3747$) (Supplementary Fig. 29, Fig. 6e), the number of prehierarchal SYF ($P = 0.0316$) and the percentage of preovulatory follicles in 22-week-old hens (Fig. 6f, g), the number of prehierarchal SWF and LWF and the ratio of preovulatory F4-F1 follicles in 24-week-old hens (Fig. 6h, i). Of note, we observed that the average laying rate from 21 to 24 weeks of age in AAV9-*APOA4* group increased by 5.99%, compared with the AAV9-NC1 group (Fig. 6j). In general, liver-specific endocrine factor *APOA4* could systematically change reproductive hormone levels and affect ovarian

follicular development to further promote early egg production in chicken.

Further, we explored the inter-tissue crosstalk mechanism between liver endocrine factor *APOA4* and HPO axis. Response tissue pathways were first evaluated by screening the top 500 genes most significantly associated with liver *APOA4* targeting hypothalamus, pituitary and ovarian tissues, respectively (Supplementary Data 27). The top 6 pathways that were most significantly enriched in each tissue pair were listed (Supplementary Table 5). We further examined the mRNA levels of 11 response genes in these pathways in *APOA4* overexpression experiment. Collagen type 1 alpha 2 chain (*COL1A2*) and collagen type IV alpha 2 chain (*COL4A2*), key genes involved in focal adhesion and ECM-receptor interaction pathway in hypothalamus, nuclear receptor coactivator 2 (*NCOA2*), a gene involved in the thyroid hormone signaling pathway in pituitary, solute carrier family 9 member A1 (*SLC9A1*) and calcium voltage-gated channel auxiliary subunit alpha2delta 1 (*CACNA2D1*), key genes involved in Adrenergic signaling in cardiomyocytes in ovary, and regucalcin (*RGN*) and prostaglandin-endoperoxide synthase 1 (*PTGSI*), key genes involved in the small molecule metabolic pathway in ovary, were significantly induced to up-regulate expression in AAV9-*APOA4* group (Supplementary Fig. 30). Of the 7 key response genes, *COL4A2*, *NCOA2* and *RGN* are GWASGs for egg production traits, and *PTGSI* is a PSG. These results indicated that hepatic *APOA4* could activate different signaling pathways and response genes in different tissues of HPO axis by inter-tissue crosstalk.

For the overexpression experiment of abdominal fat-specific *ANGPTL2* in vivo, after injection with AAV9-*ANGPTL2* virus for 10 weeks, *ANGPTL2* was most highly expressed in abdominal fat and slightly expressed in spleen, pancreas and duodenum (Fig. 6k). Both *ANGPTL2* mRNA level in abdominal fat and serum *ANGPTL2* protein level in AAV9-*ANGPTL2* group at 22 weeks of age were significantly increased compared with that in AAV9-NC2 group (Fig. 6l, m), indicating that *ANGPTL2* was successfully overexpressed in abdominal fat in the AAV9-*ANGPTL2* group. *ANGPTL2* overexpression evidently increased the serum reproductive hormone levels, ovarian index (OI), the number of prehierarchal follicles (SWF, LWF, SYF and LYF) and the percentage of preovulatory follicles in 22-week-old hens, slightly up-regulated body weight, but had no significant effect on abdominal fat percentage and liver index of hens at 22 and 24 weeks of age (Fig. 6n–q, Supplementary Fig. 31). At 24 weeks of age, the proportion of preovulatory follicles in AAV9-*ANGPTL2* group showed an increased tendency compared with AAV9-NC2 group, although no statistically significance of the difference in the number of prehierarchal follicles (Fig. 6r, s). Ultimately, overexpression of *ANGPTL2* led to 8.19% increase in the average laying rate from 21 to 24 weeks of age (Fig. 6t). Similarly, abdominal fat-specific endocrine factor *ANGPTL2* could promote chicken early egg production by systematically altering reproductive hormones and ovarian development.

The inter-tissue crosstalk mechanism between abdominal fat endocrine factor *ANGPTL2* and HPO axis were investigated. The top 500 genes most significantly associated with abdominal fat *ANGPTL2* targeting hypothalamus were used for response tissue function enrichment analysis (Supplementary Data 28), and 7 response genes in the top 6 pathways or biological processes in *ANGPTL2* overexpression experiment were observed (Supplementary Table 6), and only one gene Htra serine peptidase 1 (*HTRAI*), which was involved in cellular nitrogen compound metabolic process, was significantly induced to upregulate expression in the hypothalamus in AAV9-*ANGPTL2* group (Supplementary Fig. 32). Interestingly, *HTRAI* was also a GWASG for egg production traits. These results indicated that abdominal fat *ANGPTL2* might achieve inter-tissue crosstalk between abdominal fat and hypothalamus by activating *HTRAI* gene and cellular nitrogen compound metabolic process in hypothalamus of HPO axis.



Discussion

This study is systematically excavate small-effect and pleiotropic variations, genomic selective signals, multi-tissue HCGs, and multi-tissue key endocrine factors affecting chicken egg production by integrating multi-breed genome resequencing and multi-tissue RNA-seq data, and construct the intra-tissue molecular regulatory networks and explore the inter-tissue crosstalk of endocrine factors regulating egg-laying traits.

The egg production traits include a series of quantitative traits such as egg number and clutch size in multiple stages, and are regulated by a few large-effect variants and a large number of small-effect variants^{2,3}. And there is genetic pleiotropy among several different traits or multistage traits⁴³. These increase the difficulty for parsing their genetic regulatory mechanisms. Although previous studies have identified plenty of candidate SNPs associated with egg number through univariate SNP-based GWAS², this approach is unlikely to fully

Fig. 6 | Peripheral tissue-HPO axis crosstalk improved early egg production in Gushi chicken. **a** Tissue expression characteristics of *APOA4* in AAV9-*APOA4* group of 22-week-old Gushi hens ($n = 3$). **b, c** Liver-specific *APOA4* overexpression significantly increased its mRNA level in liver and its protein levels in serum at 22 weeks of age ($n = 9$ for each group in **(b)**; $n = 10$ for each group in **(c)**). **d–g** Effects of liver-specific *APOA4* overexpression on reproductive hormone levels, ovarian morphology, number of prehierarchal follicles and the percentage of pre-ovulatory follicles at 22 weeks of age ($n = 10$ for each group in **(d, f)**). **h, i** Effects of liver-specific *APOA4* overexpression on number of prehierarchal follicles and the percentage of pre-ovulatory follicles at 24 weeks of age ($n = 11$ for AAV9-NC1, and $n = 10$ for AAV9-*APOA4* in **(h)**). **j** Liver-specific *APOA4* overexpression affected egg number and average egg-laying rate from 21 to 24 weeks of age. **k** Tissue expression characteristics of *ANGPTL2* in AAV9-*ANGPTL2* group of 22-week-old Gushi hens

($n = 3$). **l, m** Abdominal fat-specific *ANGPTL2* overexpression significantly increased its mRNA level in liver and its protein levels in serum at 22 weeks of age ($n = 7$ for AAV9-NC2, and $n = 9$ for AAV9-*ANGPTL2*). **n–q** Effects of abdominal fat-specific *ANGPTL2* overexpression on reproductive hormone levels, ovarian morphology, number of prehierarchal follicles, and the percentage of pre-ovulatory follicles at 22 weeks of age ($n = 7$ for AAV9-NC2, and $n = 9$ for AAV9-*ANGPTL2* in **(n, p)**). **r, s** Effects of abdominal fat-specific *ANGPTL2* overexpression on number of pre-hierarchal follicles and the percentage of pre-ovulatory follicles at 24 weeks of age ($n = 8$ for AAV9-NC2, and $n = 13$ for AAV9-*ANGPTL2* in **(r)**). **t** abdominal fat-specific *ANGPTL2* overexpression affected egg number and average egg-laying rate from 21 to 24 weeks of age. Data are presented as the mean \pm SEM, and the indicated P values ($*P < 0.05$, $**P < 0.01$, and $***P < 0.001$) are based on two-tailed unpaired t -test. Source data are provided as a Source Data file.

capture the variations in regions surrounding the genotyped markers. In this study, in order to fully exploit the small-effect and pleiotropic variations driving egg production traits, in addition to SNP-based GWAS, we also comprehensively adopted haplotype-based GWAS and CCA-based GWAS to increase detection sensitivity and statistical power^{44,45}. Based on these three methods and the mining small-effect variants, the identified SNPs and haplotypes explained 35.99–64.46% of phenotypic variances for egg production traits, which partially explained the missing heritability²⁹. In addition, all large-/small-effect and pleiotropic variations significantly associated with egg production traits were widely distributed across multiple chromosomes, reflecting the micropotency of genetic regulation of egg production traits.

Both domestication and planned breeding have led to the rapid evolution of phenotypes driven by artificial selection⁸, causing the reduced genetic polymorphism or even fixed genetic allele. Comparative genomic analysis of different variety types, which enabled the identification of the selective signals in the genomic regions, accelerated the progress in solving the molecular basis of many complex phenotypic traits in agricultural animals^{46,47}. Here, by integrating the comparative study on the genomes of three chicken variety types with significant differences in egg production phenotypes and GWAS, we dissected the genetic basis explaining such large differences in egg production and identified key candidate genes affecting egg production, which is conducive to accelerating the progress of breeding selection for egg production phenotypes of local chickens. Specifically, we confirmed that *CAMK2D* is a key selected gene involved in the positive regulation of egg production in chickens by analyzing its genomic architecture and in vitro and in vivo validation.

Egg-laying regulation involves many genes across multiple tissues, including HPG axis-related tissues, liver, and abdominal fat^{15,16,48}. Recent studies have shown that some candidate causal genes associated with phenotypic traits based on genomic identification have tissue bias¹³ or tissue specificity⁴⁹. Especially for complex traits determined by minor effect genes, the efficacy of causal genes that could be detected based on a single tissue was greatly reduced⁴⁹. By combining candidate genes identified at the genome level with multi-tissue transcriptome profiles, we excavated the HCGs of hypothalamus, pituitary, ovary, liver, and abdominal fat, which are closely related to egg production, and found that these genes were mainly concentrated in ovarian, liver and abdominal fat tissues, which further indicated that the role of these peripheral tissues in the regulation of egg production should not be ignored.

We further verified the regulatory functions of HCGs in the hypothalamic and ovarian networks in vitro. Previous studies have shown that *TFPI2*, as an important serine protease inhibitor in the extracellular matrix, plays an important role in the development of the central nervous system in fish, and fetal loss of *TFPI2* can lead to serious central nervous system defects⁵⁰, indicating that *TFPI2* could be involved in the development and regulation of nerve cells. NPVF neurons, as a central regulator of bird reproduction, are located on the

hypothalamic paraventricular nucleus, secreting NPVF, and their nerve fibers can extend to median eminence to inhibit the release and secretion of GnRH by acting on GnRH neurons in the hypothalamus⁵¹. In our study, *TFPI2* overexpression could reduce *NPVF* expression and promote the GnRH secretion, but had no effect on GnRH expression in chicken primary hypothalamic neuron cells. Therefore, we speculated that *TFPI2* might partially relieve NPVF inhibition on GnRH release by decreasing *NPVF* expression, thus promoting the GnRH secretion. Meanwhile, network adjacent genes including *SLC38A4*, *ASPG*, and *FKBP5*, which play an important role in the production and release of excitatory neurotransmitters and synaptic plasticity, showed some compensatory function after *TFPI2* interference⁵². *OSTN* was previously identified as an osteoblast-derived secreted protein and promoted chondrocyte maturation and bone formation in mammals⁵³. However, its function in poultry has not been reported. In this study, in vitro test confirmed that *OSTN* may promote follicle growth and maturation by promoting granulosa cell proliferation and the synthesis of sex steroid hormones (PROG and E2). Previous studies have shown that granular layer thickness and follicle PROG levels increase significantly in the early stages of follicle selection in poultry⁵⁴, and the selected follicles eventually enter the hierarchy to form eggs, supporting the explanation that *OSTN* is involved in the positive regulation of egg production. In addition, network adjacent genes including *CCDC80*, *PTRF*, and *FBNI*, which played important regulatory functions in lipid synthesis, angiogenesis, and glycolysis⁵⁵, showed synchronous changes with *OSTN* and participated in the functional regulation of ovarian granulosa cells in different forms.

Endocrine factors perform the function of inter-tissue signal transmission. In addition to the classical reproductive endocrine factors such as hypothalamic GnRH, NPVF, VIP, and pituitary FSH, LH, PRL, a prominent instance was communication between the adipose tissue and the hypothalamus. Moreover, the perturbations of adipokine (e.g., leptin and adiponectin) in adipose tissue could affect the reproductive signal and feeding signal in the hypothalamus¹⁷. QENIE analysis can systematically establish inter-tissue communication of endocrine factors¹⁹. Cao et al.⁵⁶ first used the method to reveal the mechanism of liver endocrine factor FXI regulating liver-heart tissue communication to protect against heart failure⁵⁶. Here, QENIE analysis was used to identify key endocrine factors secreted by hypothalamus, liver and abdominal fat that affect egg production. Our study revealed some endocrine factors potentially involved in the regulation of egg production and established the peripheral tissue-HPO axis tissues crosstalk mechanism mediated by liver-derived *APOA4* or abdominal fat-derived *ANGPTL2* promoting early egg production. *APOA4* was identified as a key endocrine factor secreted from liver, and liver-specific *APOA4* overexpression could increase egg production in hens. Inter-tissue communication verification suggested that *APOA4* could realize liver-HPO axis communication by activating hypothalamic axon growth and synaptic remodeling related pathways (Focal adhesion and ECM-receptor interaction)⁵⁷, pituitary seasonal reproductive

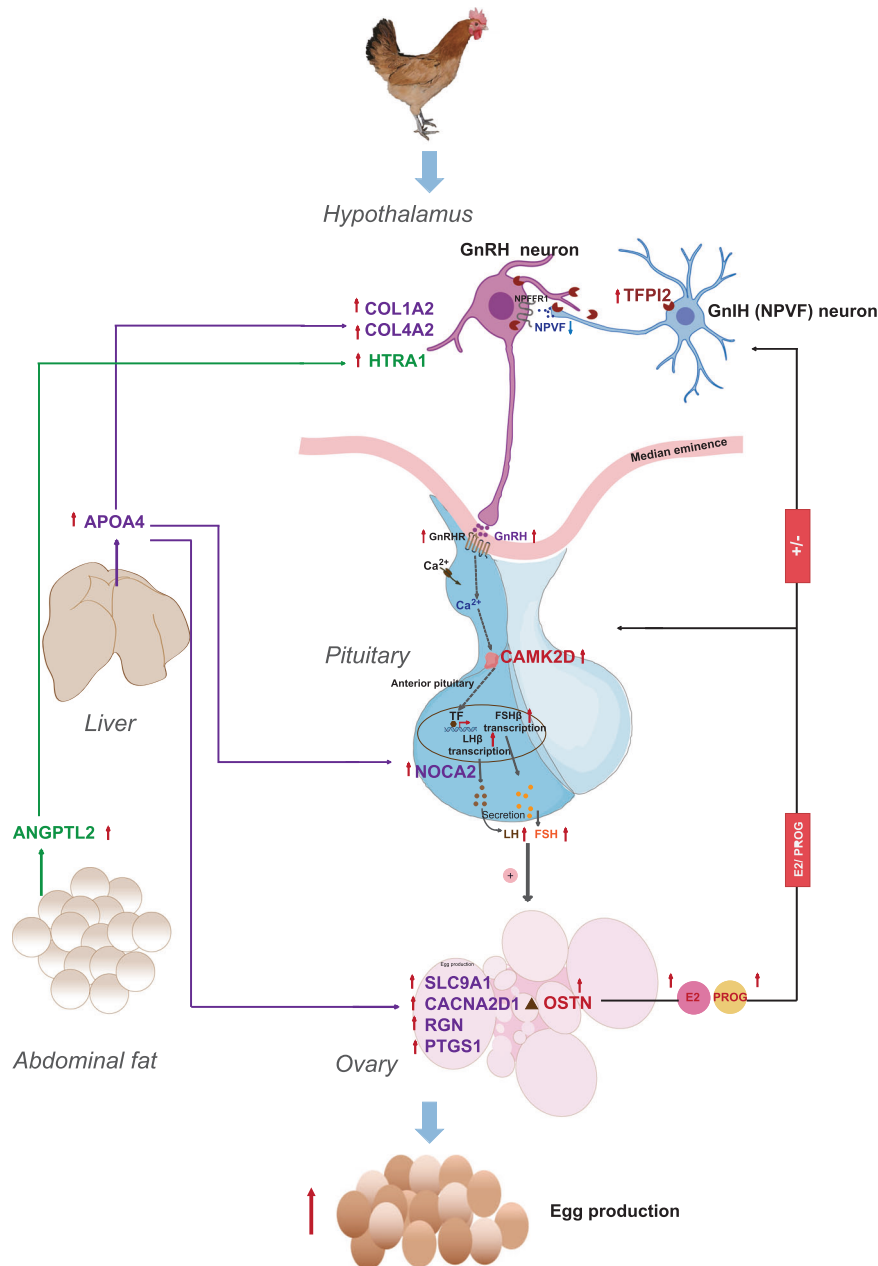


Fig. 7 | Proposed mechanism of hub candidate genes and key endocrine factors regulating chicken egg-laying phenotypes. GnRH represents gonadotropin-releasing hormone; GnIH gonadotropin-inhibiting hormone; FSH represents follicle-stimulating hormone; LH represents luteinizing hormone; E2 represents

estrogen; and PROG represents progesterone. The red up arrow indicates up-regulated expression, and the blue down arrow indicates down-regulated expression.

regulation signaling pathway (Thyroid hormone signaling pathway)⁵⁸, and ovary granulosa cell migration, Ca^{2+} homeostasis and follicle maturation related pathways (Adrenergic signaling in cardiomyocytes and small molecule metabolic process)^{59–61}. ANGPTL2, belongs to the angiopoietin-like family, was identified as a key adipokine secreted by abdominal fat. Abdominal fat-specific overexpression of ANGPTL2 could increase egg production in hens. Inter-tissue communication verification suggested that ANGPTL2 could realize abdominal fat-HPO axis communication by promoting the up-regulated expression of HTRA1 of cellular nitrogen compound metabolic process in hypothalamus to stimulate neurogenesis and neurite growth⁶².

Systematically, in combination with the functional verification of the above identified HCGs and key endocrine factors in vivo and in vitro, a proposed regulatory mechanism promoting chicken egg-

laying performance through intra-tissue and inter-tissue coordination is summarized in Fig. 7. In the regulatory system, three genes *TFPI2*, *CAMK2D* and *OSTN*, as representatives of the HCGs associated with egg production traits and selected in domestication and breeding, separately promoted the GnRH secretion in hypothalamic neuron cells, the FSH β and LH β secretion in pituitary cells, and granulosa cell proliferation and the synthesis of sex steroid hormones in ovarian granulosa cells via intra-tissue gene network interconnection. Additionally, as representatives of tissue-specific key endocrine factors, a hepatokine APOA4 and an adipokine ANGPTL2 could increase chicken egg production by inter-tissue communication with HPO axis.

In brief, all our efforts have aggregated chicken laying-related variants, superior genes and key endocrine factors. This provide a valuable resource pool for more-accurate identification of causative

variants and in-depth functional parse of egg-laying regulation at multiple levels. Construction of multi-tissue hub genetic networks and cross-tissue communication of endocrine factors broaden the horizon of research on the regulation of egg production in poultry.

Methods

Ethics statement

All animal experimental protocols were approved by the Institutional Animal Care and Use Committee of Henan Agricultural University (protocol number 11-0085). The methods were carried out in accordance with the approved guidelines.

Animals, phenotype, and sample collection

A total of 900 female individuals of Gushi chickens from the 12th generation were used for GWAS of egg production traits. The population consisted of two batches of chickens that were raised until 12 weeks of age and transferred to single cages in the same house. All individuals were raised according to the normal management standards of Gushi chickens. When reached age at first egg, all hens were recorded daily for individual egg number until 43 weeks of age. According to individual laying records, we classified the egg production traits into three categories, namely, egg number (EN), ACS, and maximum clutch size (MCS). A clutch was defined as the number of eggs laid on consecutive days without a break⁷. MCS represents maximum number of eggs in a clutch, and ACS represents average number of eggs in a clutch. According to the laying curve of Gushi chickens, we divided the whole laying period into three stages (Supplementary Fig. 33) and counted the EN and ACS in each individual phase: the early laying stage with rapid increase in egg production (the laying rate <70% from 21 to 25 weeks of age) (EN21-25w, ACS21-25w); the peak laying stage (the laying rate >70% lasting from 26 to 30 weeks of age) (EN26-30w, ACS26-30w); the decline laying stage from 31 to 43 weeks of age (EN31-43w, ACS31-43w) including the phase with 65–70% laying rate (EN31-35w, ACS31-35w) and the phase whose laying rate is lower than 65% (EN36-43w, ACS36-43w). We also calculated the total egg number (ENT) and the total average clutch size (ACST) from 21 to 43 weeks of age. Blood samples from 900 individuals at 43 weeks of age were collected by wing vein for genomic DNA extraction.

The genome resequencing data of 90 chickens from three different egg-laying types, including 50 native chicken breeds (Gushi (GS), Lushi (LS), Xichuan Black Bone (XCBB), Zhengyang San Huang (ZYSH) and Henan Gamecock (HNG) chicken²², 20 wild ancestors (Red jungle fowl, RJF)^{1,21} and 20 layer breeds (White Leghorns (WL) and Rhode Island Red (RIR) chicken¹ were used for comparative genome analysis. Among them, the data of native chickens were retrieved from our previous resequencing data²², and the data of RJF and layer breeds were downloaded from the NCBI database^{1,21}. The detailed description information was shown in Supplementary Data 7.

GS and LS chickens are the two dual-purpose egg and meat-type native breeds with similar annual egg number of 150–180 (NLPGR 2011). The female birds of both breeds were raised in single cages with the recommended conditions³⁴ after 12 weeks of age. Briefly, a common corn-soybean diet containing 12.75 MJ kg⁻¹ metabolic energy and 15.60% crude protein was provided, and the water were available *ad libitum*. HL chickens from 16 to 35 weeks of age were reared with the *ad libitum* access to water and the phased standard commercial diet of Hy-Line Brown containing 11.62–13.80 MJ kg⁻¹ metabolic energy and 16.50–17.00% crude protein (www.hyline.com). Healthy female individuals of 30-week-old GS chicken ($n = 8$), LS chicken ($n = 8$) and HL chicken ($n = 8$) were randomly selected and slaughtered humanely. Twelve type of tissues, including hypothalamus, pituitary, ovary (without follicles), cerebrum, liver, abdominal fat, pectoralis, kidney, duodenum, proventriculus, heart, and shell gland, were collected for gene expression profile analysis.

According to the individual laying records of 764 Gushi chickens from onset of laying eggs to 43 weeks of age in the 14th generation, we defined individuals whose total egg number at 20 weeks of age (EN20w) was in the top 5% of population as the 20-week-old high-yield group (GS20wH), and individuals whose EN20w was 0 as the 20-week-old low-yield group (GS20wL). And we assigned the top 10% of population with egg number as the high-yield group, and the bottom 20% of population as the low-yield group at 28, 36, and 43 weeks of age, respectively (Supplementary Fig. 9). Specifically, GS20wH group (average total EN20w with 8.92 ± 5.58) with 12 healthy individuals and GS20wL group (EN20w with 0) with 12 healthy individuals, GS28wH group (average total EN28w with 42.73 ± 4.90) with 11 healthy individuals and GS28wL group (average total EN28w with 7.62 ± 4.89) with 12 healthy individuals, GS36wH group (average total EN36w with 82.77 ± 9.96) with 13 healthy individuals and GS36wL group (average total EN36w with 40.42 ± 8.20) with 12 healthy individuals, GS43wH group (average total EN43w with 123.25 ± 13.79) with 12 healthy individuals and GS43wL group (average total EN43w with 69.50 ± 11.93) with 14 healthy individuals (Supplementary Data 15) were screened and slaughtered humanely. And serum samples were collected, carcass traits were determined and different hierarchical ovarian follicles number were counted subsequently. Tissue samples from hypothalamus, pituitary, ovary (without follicles), liver, and abdominal fat were collected and snap frozen in liquid nitrogen and stored at -80°C for subsequent transcriptome sequencing and gene expression verification. The most caudal part of the right liver lobe ($1 \times 1 \times 1$ cm) were excised and then immersed in 4% formaldehyde tissue fixating solution for hematoxylin and eosin (H&E) staining of tissue sections to determine liver lipid content (LLC).

DNA extraction and genome resequencing

Blood genomic DNA was extracted using TIANamp Genomic DNA Kit according to the manufacturer's instructions (Tiangen, Beijing, China). Genomic DNA from each sample of 900 individuals (>0.5 μg) was used to construct a paired-end sequencing library with a random DNA fragment length of ~ 150 bp. The qualified library was re-sequenced by BGISEQ sequencing platform.

Sequence read mapping

For the resequencing data of 900 GS chickens, after the raw reads were filtered, each sample ended up with ~ 6.09 Gb of high-quality clean bases, with an average depth of $5.75\times$ coverage. For the resequencing data of 90 chickens from three different egg-laying types, each sample ended up with ~ 14.65 Gb of high-quality clean bases, with an average depth of $13.82\times$ coverage. These clean reads were mapped onto the chicken reference genome (GRCg6a) with the Burrows-Wheeler Aligner (BWA v.0.7.17r1188)⁶³. Mapping results were sorted and de-duplicated using SAMtools v.1.3.1, and were reordered and calibrated for the highest quality mapping reads using GATK v3.8.

SNP calling, quality control and annotation

BaseVar-STITCH process was used for identifying polymorphic sites and imputing genotypes of the high-quality mapping data from 900 Gushi chickens⁶⁴. Subsequently, PLINK v1.90 package was implemented to control the quality of sample call rate ($>97\%$), and to filter out the low quality of SNPs including SNP call rate $<95\%$, minor allele frequency (MAF) <0.01 and Hardy-Weinberg equilibrium $P < 1 \times 10^{-6}$. Finally, a total of 888 individuals and 13,467,604 SNPs located on autosomes were qualified for the following analyses. UnifiedGenotyper of GATK v3.8 software was implemented to calling SNPs of the high-quality mapping data from 90 different breeds of chickens. The obtained SNPs were filtered by VariantFiltration of GATK v3.8 with options “QD < 4.0||FS > 60.0||MQ < 40.0||GQ < 20”. The remaining

SNPs with genotype missing rate <30% were imputed using the Beagle v5.0 procedure. Finally, a total of 21,984,699 SNPs with MAF > 0.05 were obtained using VCFtools v0.1.16. SNPs were annotated by SNPEff v 4.1 program.

SNP-based GWAS

For the 900 GS chickens, all qualified SNPs were pruned by the option of `--indep-pairwise 50 10 0.2` to obtain a total of 991,830 independent SNPs. Association analyses of egg production traits were performed using the mixed linear model (MLM) in the GCTA v1.92.2⁶⁵. The population stratification effect was corrected by adding the first three principal components (PCs) derived from the whole-genome SNPs as covariates, and the batch effect was corrected by adding the birth batch as a covariable. Based on independent SNPs, we defined SNPs as a large effect SNP and a small effect SNP with a $P < 1 \times 10^{-6}$ (1/991,830) and $P < 1 \times 10^{-4}$, respectively. The Manhattan and quantile-quantile plots of egg production traits were implemented using the “CMplot” package in the R.

Haplotype-based GWAS

Haplotype phasing and imputation were performed using Beagle v5.0 with the parameters: `beagle.jar gt=file.vcf out=file.phased gp=true`. For phased data, a total of 7065,827 SNPs was obtained by using `--indep-pairwise 50 10 0.98`, which filtered out completely linked SNPs. The whole-genome was divided into 1413,153 blocks of five successive SNPs. The haplotype-based GWAS was performed based on MLM using R package `lme4qtl v0.2.2`⁶⁶. Haplotype combinations were included as fixed effect in the model, while the random polygenic effect was captured by the genetic relationship matrix calculated using all haplotypes. Statistical significance for each haplotype block was accessed by ANOVA against the null model without the haplotype block to test for association.

CCA-based GWAS

The CCA-based GWAS is a multivariate association analysis approach that simultaneously tests the association between a single SNP and multiple genetically related phenotypes. The method is thus capable of detecting potential pleiotropic genes⁴⁵. The CCA-based GWAS was carried out by two approaches, i.e., combining same trait across different times, or combining all traits in a single time. We first computed the correlation between a SNP and multiple phenotypes, and then performed a Chi-square test on the correlation to access the significance of each SNP. The CCA was calculated by `cancor` function in R package `stats`.

Genetic parameter and variant effect

The SNP-based heritabilities and pairwise genetic correlations of egg production traits were estimated using a restricted maximum likelihood (REML) approach implemented in GCTA v1.92.2. The procedure was also used to calculate the proportion of phenotypic variance explained by the candidate SNPs and haplotypes.

Population genetics analysis

For the 90 chickens from three different egg-laying types, an individual-based NJ tree was constructed for all the samples based on the Reynolds genetic distances with 1000 bootstraps using PHYLIP v3.69, and visualized using MEGA v10.0. The whole-genome SNPs of all 90 individuals were further pruned by the option of `--indep-pairwise 50 10 0.2` by PLINK v1.90. PCA of the pruned SNPs was performed based on the genetic relationship matrix calculating by GCTA v1.92.2. The pruned SNPs were used for LD decay analysis of different varieties. The parameter R^2 for LD was calculated for pairwise SNPs using `PopLDdecay v3.41`. The average R^2 values were calculated for each length of distance. The LD decay plot was depicted against the length of distance using the R script.

Detection of selective sweeps

After filtering the sex chromosome, we generated a final set of 10054,021 SNPs located on autosomes for detecting the selective sweeps. Two approaches including F_{ST} and the comparison of nucleotide diversity (π) ratios ($\log_2(\pi\text{-ratio})$) were used for performing tests of selective sweeps during domestication and breeding of native chicken breeds and layer breeds. F_{ST} approach implemented in `vcftools v0.1.16` and was used to test the degree of population genetic differentiation, while $\log_2(\pi\text{-ratio})$ was also calculated in `vcftools v0.1.16` and was used to test the degree of nucleotide diversity of a genomic region⁸. Values of F_{ST} and π were calculated with a 40 kb sliding window and a 10 kb sliding step. F_{ST} values were changed using Z-transform (ZF_{ST}). In each comparison, the genomic regions in the top 5% ZF_{ST} values and $\log_2(\pi\text{-ratio})$ values across the whole-genome were considered to be the candidate selective genomic region.

Measurements of serum reproductive hormone concentrations

The concentrations of serum reproductive hormones including FSH, LH, E2, PROG, and PRL in all the above slaughtered high- and low-yield GS chickens at 20, 28, 36, and 43 weeks of age were measured by using the corresponding chicken Enzyme Linked Immunosorbent Assay Kit (Jiangsu Meimian industrial Inc., China), respectively, according to the manufacturer's instructions. Three technological duplications were performed for each reproductive hormone in each serum sample.

Multi-tissue transcriptome profiling

A total of 80 samples from five tissue types (hypothalamus, pituitary, ovary, liver and abdominal fat) of 43-week-old Gushi hens from high- (GS43wH, $n = 8$) and low-yield group (GS43wL, $n = 8$) were collected for RNA-Seq analysis. The total RNA from all 80 tissues were extracted using Trizol RNA Reagent (Takara, Dalian, China). A total of 78 RNA samples (14 from hypothalamus and 16 from each of the other 4 tissues) were qualified for the construction of cDNA libraries and sequenced using the Illumina Novaseq 6000 System (Illumina, San Diego, CA) to generate 150-bp paired-end reads. Clean reads were aligned to the chicken galGal 6 reference genome using HISAT2. Transcript abundance was calculated using RSEM and normalized via FPKM method.

WGCNA

To identify genes sets responsible for egg number and serum reproductive hormones in five tissues, a co-expression network analysis was performed using the WGCNA package⁶⁷ in R. The network was constructed using topology overlap matrix, module detection, and similar module merging functions. The minimal module size was set to 50. Egg production traits including ENT, EN39-43w, FSH, LH, E2, and PROG were used as trait files to evaluate module-trait relationships. Significant correlations between modules and traits were defined as $P < 0.05$, where * represents $P < 0.05$, ** for $P < 0.01$, and *** for $P < 0.001$. For each of the significantly correlated modules, the genes with gene significance (GS, $|GS| > 0.5$, $P < 0.05$) and module membership (MM, $|MM| > 0.5$, $P < 0.05$) were identified as modules hub genes (MHGs).

Differential expression analysis

DESeq2 were used for differential expression analysis between high- and low-yield group. Benjamini-Hochberg method was used to calculate the adjusted P value (FDR) for multiple testing corrections. The DEGs were identified according to the criteria of $FPKM \geq 1$, $|\text{fold change}| \geq 1.5$ and $q < 0.05$.

Molecular network construction and functional enrichment of module hub genes

By combining the gene correlation weight, gene connectivity, whether a gene was a differential MHG, and whether a gene is a HCG or a KCG,

we constructed molecular co-expression regulatory networks of hub genes associated with egg-laying phenotypes based on the most significant positive and negative correlation modules in the five tissue types. Cytoscape was used for visualization of molecular network construction. The putative functions of module hub genes were investigated by gene ontology (GO) enrichment analysis with R package clusterProfiler at a significance level of P value < 0.05 .

Plasmid construction and siRNA synthesis for in vitro validation

Gene overexpression plasmids were constructed by homologous recombination method, *TFPI2* and *OSTN* were cloned into the pcDNA3.1-EGFP (Invitrogen, Carlsbad, CA) vector and pcDNA3.1- $3 \times$ flag vector (Invitrogen, Carlsbad, CA), respectively. The siRNA oligonucleotides specifically against chicken *CAMK2D*, *TFPI2* and *OSTN* (si-CAMK2D, si-TFPI2 and si-OSTN), respectively and a nonspecific duplex (si-NC, negative control) were synthesized from GenePharma Co., Ltd. (Shanghai, China).

Chicken pituitary cell culture, induction and transfection

The pituitaries isolated from 17-day-old chicken embryos were washed for three times with PBS containing 1 mg/ml bovine serum albumin and 1% penicillin/streptomycin, and cut into pieces. The digested cell suspension with 1 mg/ml collagenase type II (Solarbio, Beijing, China) was filtered using 200-mesh screens, then centrifuged at 1500 rpm for 8 min. The re-suspended pituitary cells were cultured at a density of 5×10^5 cells per well in DMEM (Gibco, Gaithersburg, MD) supplemented with 5% fetal bovine serum (FBS) (Gibco, Gaithersburg, MD), 500 μ g/ml transferrin, 500 μ g/ml bovine insulin and 1% penicillin/streptomycin in a 24-well plate (NUNC) at 37 °C with 5% CO₂.

After 24 h incubation at 37 °C, the medium was replaced by 500 μ l DMEM containing 0 nM, 25 nM, and 50 nM GnRH agonist (Alarelin acetate) (MCE) and incubated for 12 h or 24 h. Each treatment contained 4 biological replicates. After treatment, cell supernatant was collected for determination of FSH β and LH β hormone levels, and cell precipitation was collected for RNA extraction to determine gene expression. si-CAMK2D and si-NC were transfected into pituitary cells after 12 h incubation with 25 nM GnRH agonist. After 24 h of treatment, cells were collected for testing the *CAMK2D* interference efficiency and the mRNA levels of genes involved in hormone synthesis.

Chicken primary hypothalamic neuron cell culture and transfection

The hypothalamuses isolated from 17-day-old chicken embryos were shredded, digested with 1 mg/ml collagenase type II, and filtered using 200-, 500-mesh sieves, respectively. The filtered cell suspension was centrifuged for three times at $150 \times g$ for 7 min, then re-suspended by DMEM supplemented with 15% FBS, 1% L-glutamine (Solarbio, Beijing, China) and 1% penicillin/streptomycin. The re-suspended cells were cultured at a density of 1×10^6 cells per well in a 5% polylysine (Sigma) coated 12-well plate (NUNC) at 37 °C with 5% CO₂. After 36 h incubation, the medium was replaced by Neurobasal medium (Gibco, Gaithersburg, MD) supplemented with 1% L-glutamine, 2% B27 (Gibco, Gaithersburg, MD), 1% penicillin/streptomycin and 5% β -D-cytarabine (Solarbio, Beijing, China), then replaced by Neurobasal medium without β -D-cytarabine after 24 h incubation. Subsequently, overexpression and knockdown experiments of the *TFPI2* were performed using the transfection reagent Lipofectamine 3000 (Invitrogen, Carlsbad, CA) following the manufacturer's instruction, respectively.

Chicken granulosa cell culture and transfection

The stratum granulosa of the 6–12 mm follicles separated from 30-week-old hens was cut into pieces. The granular layer suspension was digested with 1 mg/ml collagenase type II after which it was filtered through a 200-mesh sieve, then resuspended and plated with DMEM

(VivaCell, Shanghai, China) containing 5% FBS and 1% penicillin/streptomycin. The granulosa cells were incubated at 37 °C with 5% CO₂. After 12–14 h incubation, overexpression and knockdown experiments of the *OSTN* gene were performed using the transfection reagent LipofectamineLTX (Invitrogen, Carlsbad, CA).

CCK-8 assay

Granulosa cells cultured in 96-well plates were transfected with the overexpressed plasmids (pcDNA3.1-OSTN and pcDNA3.1-EGFP) and siRNA oligonucleotides (si-OSTN and si-NC), respectively. Cell proliferation was evaluated at 12, 24, and 36 h after transfection using cell counting kit-8 (CCK-8) reagent (Dojindo, Kumamoto, Japan) according to the instruction.

Real-time quantitative PCR, western blot, and immunofluorescence

The mRNA expression changes of genes in vivo or in vitro were examined using real-time quantitative PCR (qRT-PCR). The specific primers used for qRT-PCR were designed using NCBI Primer-BLAST tool (Supplementary Tables 7–9). qRT-PCR reaction was implemented in LightCycler 96 Instrument (Roche Applied Science, IN) with $2 \times$ SYBR Premix Ex TaqTM II (TaKaRa). Each sample was tested in triplicate. The relative mRNA level of gene was calculated using the $2^{-\Delta\Delta Ct}$ method and normalized by the internal control *GAPDH* gene.

Protein was extracted from the transfected cells using RIPA Lysis buffer (Beyotime, Shanghai, China) and was quantified by BCA protein quantification kit (Thermo Fisher, Shanghai, China). The western blot (WB) was implemented as follows: The denatured protein (50 μ g) was separated on a 10% SDS-PAGE gel and transferred to a methanol-activated polyvinylidene difluoride (PVDF) membrane (Millipore, Danvers, MA). The membrane was then blocked with 5% nonfat milk and incubated overnight at 4 °C with the primary antibodies of rabbit anti-TFPI2 (1:500; chicken peptide sequence:CAALAPRGLTEKQR, Homemade antibody)⁶⁸, Polyclonal anti-CYP11A1 (1:2000, 13363-1-AP, Proteintech, Wuhan, China), rabbit anti-CYP19A1 (1:1000, A12684, ABclonal, Wuhan, China), rabbit anti-STAR (1:1000, A16432, ABclonal, Wuhan, China) and mouse anti-GAPDH (1:50000, 60004-1-Ig, Proteintech, Wuhan, China), respectively. Then, the membrane was incubated with the secondary antibody (1:50000, 5220-0336, SeraCare, Beijing, China) for 1 h at room temperature. The signal of WB was detected with an enhanced chemiluminescence system (Odyssey Fc, LI-COR, Lincoln, NE). The gray values of the blot signals were counted using ImageJ software (NIH, Bethesda, Maryland, USA). The protein level of gene was normalized to the loading control GAPDH. Polyclonal antibodies against GnRH (1:500, PAA843Ga01, Cloud-clone, Wuhan, China) and FSHR (1:200, A3172, ABclonal, Wuhan, China) were used to identify chicken primary hypothalamic neuron cells and chicken ovarian granulosa cells via immunofluorescence assay. The immunofluorescence images were captured by using fluorescence microscope (Olympus, Melville, NY, USA).

QENIE analysis

According to the implementation method of QENIE¹⁹, we first constructed cross-tissue biweight midcorrelation matrices between endocrine factors of origin tissue and genes of target tissue, and calculated the correlation coefficients (bicor) and Student's correlation P value between genes. The $-\ln(P)$ of endocrine genes in each tissue of origin was further calculated and corrected by the number of transcripts in the target tissue. We further assessed the cross-tissue predictive strength (Ssec) of each origin endocrine factors by computing the sum of the $-\ln(P)$ for each origin endocrine factors across all target tissue transcripts¹⁹. In addition, we retained the top 500 genes in the target tissue that were most significantly associated with each origin endocrine factor for interrogating cross-tissue enrichment of biological function.

Tissue-specific endocrine factor overexpression test in chickens

Liver-specific overexpression recombinant AAV9 vector of chicken APOA4 (AAV9-TBG-APOA4-ZsGreen) and abdominal fat-specific overexpression recombinant AAV9 vector (AAV9-FABP4-ANGPTL2-ZsGreen) were constructed, packaged, and purified by Hanbio Biotechnology (Shanghai, China). The titer of the purified virus was 1×10^{12} vg/ml. A total of 120 healthy 12-week-old Gushi pullets with similar body weight were selected for the experiment, with 30 individuals in each group.

AAV9-TBG-ZsGreen (AAV9-NC1) and AAV9-TBG-APOA4-ZsGreen (AAV9-APOA4) were used to test for liver-specific APOA4 overexpression, while AAV9-FABP4-ZsGreen (AAV9-NC2) and AAV9-FABP4-ANGPTL2-ZsGreen (AAV9-ANGPTL2) were used to test for abdominal fat-specific ANGPTL2 overexpression. A total of 200 μ l virus was injected into each individual with an average weight of 800 g by in situ liver injection and intraperitoneal injection, respectively. After injection, Gushi pullets were fed normally until 24 weeks of age, during which the body weight and egg production of each group were estimated. The experimental population were slaughtered humanely at 22 and 24 weeks of age, respectively, in which 10 individuals were slaughtered in each group at 22-week of age and the remaining individuals in each group at 24 weeks of age. The serum samples were collected, carcass traits including AFP, LI, and OI were measured, the number of prehierarchal follicles and the proportion of preovulatory follicles were counted. Additionally, 11 types of tissues, including hypothalamus, pituitary, ovary, liver, abdominal fat, kidney, duodenum, pectoralis, leg muscle, pancreas, and spleen, were rapidly collected and stored.

Detecting the expression of APOA4, ANGPTL2, and their response genes

Total RNA was extracted from 11 tissues of 22-week-old AAV9-APOA4 group and AAV9-ANGPTL2 group for detecting tissue specific expressions of APOA4 and ANGPTL2 by qRT-PCR. Total RNA was extracted from liver tissues of AAV9-NC1 and AAV9-APOA4 groups, and abdominal fat tissues of AAV9-NC2 and AAV9-ANGPTL2 groups at 22 weeks of age for detecting the expression differences of liver APOA4 and abdominal fat ANGPTL2 between the two groups. The serum protein levels of endocrine factors between the two groups were determined by chicken APOA4 and ANGPTL2 ELISA kit (Jiangsu Meimian Industrial Inc, Jiangsu, China), respectively. Total RNA from hypothalamus, pituitary, ovary, liver, abdominal fat, duodenum, and kidney of the four groups at 22 weeks of age were used for detecting the tissue specific differential expression of liver APOA4 targeted-response genes in HPO axis and abdominal fat ANGPTL2 targeted-response genes in hypothalamus. Primer information were list in Supplementary Table 9.

Reporting summary

Further information on research design is available in the Nature Portfolio Reporting Summary linked to this article.

Data availability

The resequenced raw data from 888 Gushi hens were deposited in the Genome Sequence Archive (GSA) with accession number [PRJCA021392](https://www.genome.gov/PRJCA021392). The RNA-seq raw data of 5 tissue types were deposited in NCBI Sequence Read Archive with accession number [PRJNA893445](https://www.ncbi.nlm.nih.gov/PRJNA893445) and [PRJNA953784](https://www.ncbi.nlm.nih.gov/PRJNA953784). All other data supporting the findings of this study are available within the article and its Supplementary Information files. A reporting summary for this Article is available as a Supplementary Information file. Source data are provided with this paper.

References

- Qanbari, S. et al. Genetics of adaptation in modern chicken. *PLoS Genet.* **15**, e1007989 (2019).

- Du, Y. et al. Endocrine and genetic factors affecting egg laying performance in chickens: a review. *Br. Poult. Sci.* **61**, 538–549 (2020).
- Wolc, A. et al. Investigating the genetic determination of clutch traits in laying hens. *Poult. Sci.* **98**, 39–45 (2019).
- Gao, J. et al. Genome-wide association study of egg-laying traits and egg quality in Lingkun chickens. *Front. Vet. Sci.* **9**, 877739 (2022).
- Zhao, X. et al. Identification of candidate genomic regions for chicken egg number traits based on genome-wide association study. *BMC Genom.* **22**, 610 (2021).
- Ding, J. et al. A significant quantitative trait locus on chromosome Z and its impact on egg production traits in seven maternal lines of meat-type chicken. *J. Anim. Sci. Biotechnol.* **13**, 96 (2022).
- Wolc, A. et al. Genome-wide association study for egg production and quality in layer chickens. *J. Anim. Breed. Genet.* **131**, 173–182 (2014).
- Rubin, C. J. et al. Whole-genome resequencing reveals loci under selection during chicken domestication. *Nature* **464**, 587–591 (2010).
- Wang, M. S. et al. 863 genomes reveal the origin and domestication of chicken. *Cell Res.* **30**, 693–701 (2020).
- Li, J. et al. Novel regulatory factors in the hypothalamic-pituitary-ovarian axis of hens at four developmental stages. *Front. Genet.* **11**, 591672 (2020).
- Mishra, S. K. et al. Transcriptome analysis reveals differentially expressed genes associated with high rates of egg production in chicken hypothalamic-pituitary-ovarian axis. *Sci. Rep.* **10**, 5976 (2020).
- Li, D. et al. Dynamic transcriptome and chromatin architecture in granulosa cells during chicken folliculogenesis. *Nat. Commun.* **13**, 131 (2022).
- Wainberg, M. et al. Opportunities and challenges for transcriptome-wide association studies. *Nat. Genet.* **51**, 592–599 (2019).
- Yang, X. Multitissue multiomics systems biology to dissect complex diseases. *Trends Mol. Med.* **26**, 718–728 (2020).
- Gloux, A. et al. Integrative analysis of transcriptomic data related to the liver of laying hens: from physiological basics to newly identified functions. *BMC Genom.* **20**, 821 (2019).
- Bornelöv, S. et al. Comparative omics and feeding manipulations in chicken indicate a shift of the endocrine role of visceral fat towards reproduction. *BMC Genom.* **19**, 295 (2018).
- Fontana, R. & Della Torre, S. The deep correlation between energy metabolism and reproduction: a view on the effects of nutrition for women fertility. *Nutrients* **8**, 87 (2016).
- Wang, G. X. et al. The brown fat-enriched secreted factor Nrg4 preserves metabolic homeostasis through attenuation of hepatic lipogenesis. *Nat. Med.* **20**, 1436–1443 (2014).
- Seldin, M. M. et al. A strategy for discovery of endocrine interactions with application to whole-body metabolism. *Cell Metab.* **27**, 1138–1155.e6 (2018).
- Li, C. et al. Expression and localization of adiponectin and its receptors (AdipoR1 and AdipoR2) in the hypothalamic-pituitary-ovarian axis of laying hens. *Theriogenology* **159**, 35–44 (2021).
- Wang, M. S. et al. Genomic analyses reveal potential independent adaptation to high altitude in Tibetan chickens. *Mol. Biol. Evol.* **32**, 1880–1889 (2015).
- Zhi, Y. et al. Genome-wide genetic structure of Henan indigenous chicken breeds. *Animals* **13**, 753 (2023).
- Sutter, N. B. et al. A single IGF1 allele is a major determinant of small size in dogs. *Science* **316**, 112–115 (2007).
- Stoffel, W. et al. Neutral sphingomyelinase (SMPD3) deficiency disrupts the Golgi secretory pathway and causes growth inhibition. *Cell Death Dis.* **7**, e2488 (2016).

25. Haisenleder, D. J., Ferris, H. A. & Shupnik, M. A. The calcium component of gonadotropin-releasing hormone-stimulated luteinizing hormone subunit gene transcription is mediated by calcium/calmodulin-dependent protein kinase type II. *Endocrinology* **144**, 2409–2416 (2003).
26. Han, S. J. et al. Protein kinase B/Akt phosphorylation of PDE3A and its role in mammalian oocyte maturation. *Embo. J.* **25**, 5716–5725 (2006).
27. Bello, S. F. et al. Research Note: Association of single nucleotide polymorphism of AKT3 with egg production traits in White Muscovy ducks (*Cairina moschata*). *Poult. Sci.* **101**, 102211 (2022).
28. Miao, H., Miao, C. X., Li, N. & Han, J. FOXJ2 controls meiosis during spermatogenesis in male mice. *Mol. Reprod. Dev.* **83**, 684–691 (2016).
29. Boyle, E. A., Li, Y. I. & Pritchard, J. K. An expanded view of complex traits: from polygenic to omnigenic. *Cell* **169**, 1177–1186 (2017).
30. Xie, Q. et al. The role of kisspeptin in the control of the hypothalamic-pituitary-gonadal axis and reproduction. *Front. Endocrinol. (Lausanne)* **13**, 925206 (2022).
31. Lee, K. A., Volentine, K. K. & Bahr, J. M. Two steroidogenic pathways present in the chicken ovary: theca layer prefers delta 5 pathway and granulosa layer prefers delta 4 pathway. *Domest. Anim. Endocrinol.* **15**, 1–8 (1998).
32. Craig, J. et al. Gonadotropin and intra-ovarian signals regulating follicle development and atresia: the delicate balance between life and death. *Front. Biosci.* **12**, 3628–3639 (2007).
33. Li, S. et al. VIP activates primordial follicles of rat through ERK-mTOR pathway in tissue culture. *Reproduction* **157**, 475–484 (2019).
34. Wang, D. D. et al. Integrative analysis of hypothalamic transcriptome and genetic association study reveals key genes involved in the regulation of egg production in indigenous chickens. *J. Integ. Agric.* **21**, 1457–1474 (2022).
35. Rydze, R. T. et al. Deletion of gremlin-2 alters estrous cyclicity and disrupts female fertility in mice. *Biol. Reprod.* **105**, 1205–1220 (2021).
36. Kamkrathok, B., Sartsoongnoen, N., Chaiseha, Y. & Neuropeptide, Y. and maternal behavior in the female native Thai chicken. *Acta Histochem.* **123**, 151698 (2021).
37. Reid, A. M. A. et al. Pancreatic PYY but not PPY expression is responsive to short-term nutritional state and the pancreas constitutes the major site of PYY mRNA expression in chickens. *Gen. Comp. Endocrinol.* **252**, 226–235 (2017).
38. Jais, A. et al. PNOC^{ARC} neurons promote hyperphagia and obesity upon high-fat-diet feeding. *Neuron* **106**, 1009–1025.e10 (2020).
39. Simon, Á. et al. Changes in expression of neuropeptides and their receptors in the hypothalamus and gastrointestinal tract of calorie restricted hens. *Acta Biol. Hung.* **68**, 237–247 (2017).
40. Boswell, T. & Dunn, I. C. Regulation of the avian central melanocortin system and the role of leptin. *Gen. Comp. Endocrinol.* **221**, 278–283 (2015).
41. Li, S. et al. GDF10 is a signal for axonal sprouting and functional recovery after stroke. *Nat. Neurosci.* **18**, 1737–1745 (2015).
42. Xu, C. et al. Wif1 mediates coordination of bone morphogenetic protein and Wnt signaling in neural and glioma stem cells. *Cell Transplant.* **31**, 9636897221134540 (2022).
43. Dong, X. et al. Genomic analysis reveals pleiotropic alleles at EDN3 and BMP7 involved in chicken comb color and egg production. *Front. Genet.* **10**, 612 (2019).
44. Howard, D. M. et al. Genome-wide haplotype-based association analysis of major depressive disorder in Generation Scotland and UK Biobank. *Transl. Psychiatry* **7**, 1263 (2017).
45. Tang, C. S. & Ferreira, M. A. R. A gene-based test of association using canonical correlation analysis. *Bioinformatics* **28**, 845–850 (2012).
46. Zhou, Z. et al. An intercross population study reveals genes associated with body size and plumage color in ducks. *Nat. Commun.* **9**, 2648 (2018).
47. Li, X. et al. Whole-genome resequencing of wild and domestic sheep identifies genes associated with morphological and agronomic traits. *Nat. Commun.* **11**, 2815 (2020).
48. Zhang, X. Y. et al. Genetic selection on abdominal fat content alters the reproductive performance of broilers. *Animal* **12**, 1232–1241 (2018).
49. Li, B. et al. Influence of tissue context on gene prioritization for predicted transcriptome-wide association studies. *Pac. Symp. Biocomput.* **24**, 296–307 (2019).
50. Zhang, Y. et al. Tissue factor pathway inhibitor-2: A novel gene involved in zebrafish central nervous system development. *Dev. Biol.* **381**, 38–49 (2013).
51. Tsutsui, K., Ubuka, T. & Ukena, K. Advancing reproductive neuroendocrinology through research on the regulation of GnIH and on its diverse actions on reproductive physiology and behavior. *Front. Neuroendocrinol.* **64**, 100955 (2022).
52. Dooley, C. M. et al. The gene regulatory basis of genetic compensation during neural crest induction. *PLoS Genet.* **15**, e1008213 (2019).
53. Watanabe-Takano, H. et al. Mechanical load regulates bone growth via periosteal Osteocrin. *Cell. Rep.* **36**, 109380 (2021).
54. Nie, R. et al. Morphological characteristics and transcriptome landscapes of chicken follicles during selective development. *Animals* **12**, 713 (2022).
55. Handa, T. et al. Osteocrin ameliorates adriamycin nephropathy via p38 mitogen-activated protein kinase inhibition. *Sci. Rep.* **11**, 21835 (2021).
56. Cao, Y. et al. Liver-heart cross-talk mediated by coagulation factor XI protects against heart failure. *Science* **377**, 1399–1406 (2022).
57. Kerrisk, M. E., Cingolani, L. A. & Koleske, A. J. ECM receptors in neuronal structure, synaptic plasticity, and behavior. *Prog. Brain Res.* **214**, 101–131 (2014).
58. Shinomiya, A., Shimamura, T., Nishiwaki-Ohkawa, T. & Yoshimura, T. Regulation of seasonal reproduction by hypothalamic activation of thyroid hormone. *Front. Endocrinol.* **5**, 12 (2014).
59. Jensen, H. H. et al. The Na⁺/H⁺ exchanger NHE1 localizes as clusters to cryptic lamellipodia and accelerates collective epithelial cell migration. *J. Physiol.* **597**, 849–867 (2019).
60. Marques, R., Maia, C. J., Vaz, C., Correia, S. & Socorro, S. The diverse roles of calcium-binding protein regucalcin in cell biology: from tissue expression and signalling to disease. *Cell. Mol. Life Sci.* **71**, 93–111 (2014).
61. Fayad, T., Lévesque, V., Sirois, J., Silversides, D. W. & Lussier, J. G. Gene expression profiling of differentially expressed genes in granulosa cells of bovine dominant follicles using suppression subtractive hybridization. *Biol. Reprod.* **70**, 523–533 (2004).
62. Muñoz, S. S. et al. The serine protease HtrA1 contributes to the formation of an extracellular 25-kDa apolipoprotein E fragment that stimulates neurogenesis. *J. Biol. Chem.* **293**, 4071–4084 (2018).
63. Li, H. & Durbin, R. Fast and accurate short read alignment with Burrows-Wheeler transform. *Bioinformatics* **25**, 1754–1760 (2009).
64. Yang, R. et al. Accelerated deciphering of the genetic architecture of agricultural economic traits in pigs using a low-coverage whole-genome sequencing strategy. *GigaScience* **10**, giab048 (2021).
65. Zhang, Y. et al. Genome-wide association study reveals the genetic determinism of growth traits in a Gushi-Anka F2 chicken population. *Heredity* **126**, 293–307 (2021).
66. Ziyatdinov, A. et al. lme4qtl: linear mixed models with flexible covariance structure for genetic studies of related individuals. *BMC Bioinform.* **19**, 68 (2018).

67. Langfelder, P. & Horvath, S. WGCNA: an R package for weighted correlation network analysis. *BMC Bioinform.* **9**, 559 (2008).
68. Li, C. et al. Expression of tissue factor pathway inhibitor 2 in the follicles of chicken ovaries and its regulatory mechanism in cultured granulosa cells. *J. Integr. Agr.* <https://doi.org/10.1016/j.jia.2023.06.038> (2023).

Acknowledgements

This study was supported by the National Key Research and Development Program (2022YFF1000202), the National Natural Science Foundation of China (32272867), Key Project of NSFC-Henan Province Joint Grand (U1704233).

Author contributions

D.W. performed the majority of experiments and drafted the manuscript. D.W., L.T., Y.Z., and L.B. performed computational analysis and explained the results. Y.W. and C.X. managed the experimental animals and collected samples. Y.W., Z.W., and Y.G. constructed expression vectors and performed cell transfection study. W.T., D.L., Z.L., R.J., and R.H. performed in vivo study and bioinformatics analysis. G.L., Y.W., and Y.T. analyzed the results and participated in critical discussions. D.X. and I.C.D. implemented the article revision. X.H., H.L., Y.Z., X.K., and X.L. participated in experimental design and critical discussions. H.L. and X.L. conceived the study, revised the manuscript, and provided overall supervision. All authors read and approved the final manuscript.

Competing interests

The authors declare no competing interests.

Additional information

Supplementary information The online version contains supplementary material available at <https://doi.org/10.1038/s41467-024-50809-9>.

Correspondence and requests for materials should be addressed to Hong Li, Yiqiang Zhao, Xiangtao Kang or Xiaojun Liu.

Peer review information *Nature Communications* thanks Yiping Liu, and the other, anonymous, reviewer for their contribution to the peer review of this work. A peer review file is available.

Reprints and permissions information is available at <http://www.nature.com/reprints>

Publisher's note Springer Nature remains neutral with regard to jurisdictional claims in published maps and institutional affiliations.

Open Access This article is licensed under a Creative Commons Attribution-NonCommercial-NoDerivatives 4.0 International License, which permits any non-commercial use, sharing, distribution and reproduction in any medium or format, as long as you give appropriate credit to the original author(s) and the source, provide a link to the Creative Commons licence, and indicate if you modified the licensed material. You do not have permission under this licence to share adapted material derived from this article or parts of it. The images or other third party material in this article are included in the article's Creative Commons licence, unless indicated otherwise in a credit line to the material. If material is not included in the article's Creative Commons licence and your intended use is not permitted by statutory regulation or exceeds the permitted use, you will need to obtain permission directly from the copyright holder. To view a copy of this licence, visit <http://creativecommons.org/licenses/by-nc-nd/4.0/>.

© The Author(s) 2024